Climate of the Neoproterozoic

Article *in* Annual Review of Earth and Planetary Sciences · May 2011

DOI: 10.1146/annurev-earth-040809-152447

4 authors, including:

Aiko Voigt
Karlsruhe Institute of Technology
38 PUBLICATIONS **756** CITATIONS

Climate of the Neoproterozoic

R.T. Pierrehumbert,[1] D.S. Abbot,[1] A. Voigt,[2] and D. Koll[3]

[1]Department of Geophysical Sciences, University of Chicago, Chicago, Illinois 60637; email: rtp1@geosci.uchicago.edu

[2]Max-Planck-Institut für Meteorologie, 20146 Hamburg, Germany

[3]Department of Earth and Planetary Sciences, Harvard University, Cambridge, Massachusetts 02138

Annu. Rev. Earth Planet. Sci. 2011. 39:417–60

The *Annual Review of Earth and Planetary Sciences* is online at earth.annualreviews.org

This article's doi:
10.1146/annurev-earth-040809-152447

0084-6597/11/0530-0417$20.00

Keywords

Snowball Earth, Cryogenian, carbon cycle, astrobiology, habitability

Abstract

The Neoproterozoic is a time of transition between the ancient microbial world and the Phanerozoic, marked by a resumption of extreme carbon isotope fluctuations and glaciation after a billion-year absence. The carbon cycle disruptions are probably accompanied by changes in the stock of oxidants and connect to glaciations via changes in the atmospheric greenhouse gas content. Two of the glaciations reach low latitudes and may have been Snowball events with near-global ice cover. This review deals primarily with the Cryogenian portion of the Neoproterozoic, during which these glaciations occurred. The initiation and deglaciation of Snowball states are discussed in light of a suite of general circulation model simulations designed to facilitate intercomparison between different models. Snow cover and the nature of the frozen surface emerge as key factors governing initiation and deglaciation. The most comprehensive model discussed confirms the possibility of initiating a Snowball event with a plausible reduction of CO_2. Deglaciation requires a combination of elevated CO_2 and tropical dust accumulation, aided by some cloud warming. The cause of Neoproterozoic biogeochemical turbulence, and its precise connection with Snowball glaciations, remains obscure.

1. INTRODUCTION

Phanerozoic: the time from 542 million years ago to the present, during which abundant animal life appears in the fossil record

Metazoa: multicellular animal life

Cryogenian: the portion of the Neoproterozoic containing the major glaciations

Snowball state: a state in which oceans are completely covered with ice, all the way to the equator

Waterbelt (formerly Soft Snowball or Slushball) state: a state with low-latitude ice margins but a substantial band of open water in the tropics

The Neoproterozoic is the era extending from 1,000 million years ago (1,000 Mya) to 540 million years ago (540 Mya), a stretch of time essentially as long as the Phanerozoic. Until near the end of the Neoproterozoic, however, much of the Neoproterozoic show played out on the microbial stage and was recorded only dimly in the fossil record. The Neoproterozoic is like a dark tunnel. The ancient microbial world enters the far end, endures the biogeochemical and climatic turbulence of the Neoproterozoic, and comes out into the light of the metazoan-rich Phanerozoic world on the other side.

The middle of the Neoproterozoic marks the return of glaciation to Earth after a billion-year absence, which is why this span is sometimes termed the Cryogenian. In two of these glaciations, there were continental ice sheets in low latitudes, and a plausible case can be made that the oceans were almost entirely frozen over. This state of affairs is known as a Snowball Earth and has sparked much intense inquiry. Much discussion of the Neoproterozoic has focused on the Snowball Earth question. However, biogeochemical proxies for the Neoproterozoic show that there was a lot more going on at the time than just the charismatic Snowball-type events. The nominal Snowball events may indeed be just one of the more visible manifestations of the general biogeochemical turbulence of the Neoproterozoic. The Phanerozoic seems, by comparison, to be a rather quiescent place. Is the biogeochemical *sturm und drang* of the Neoproterozoic safely behind us? Is it that the biogeochemical cycling associated with complex biota has somehow stabilized the Earth system (at least up until technological life came on the scene)? Or does the settling down of the Earth system into a comfortable middle age have more to do with Earth's long-term geological evolution than with the emergence of complex life forms? A better understanding of the Neoproterozoic would put us in a position to approach such deep questions.

In this review, we are principally concerned with the climate dynamics of the Cryogenian and with aspects of the geological and biogeochemical record that have a bearing on climate. For a more comprehensive review of the geological record, the reader is referred to reviews by Hoffman & Li (2009), Fairchild & Kennedy (2007), and Hoffman & Schrag (2002). The Neoproterozoic glaciations provide the main indication of climate variability, but apart from that and the broad inferences that can be drawn from survival of various forms of marine life, there are no proxies to tell us how hot it may have been between glaciations. The biogeochemical picture, along with general background information relevant to climate simulations, is discussed in Section 2. Given the nature of the data, the prime targets for climate theorists dealing with the Neoproterozoic have been the explanation of the onset and terminations of the major glaciations and the manner in which these are manifest in the sedimentary record. In this review, the term Snowball refers to a situation in which the oceans are globally frozen over, except perhaps for limited and intermittent open-water oases; in the literature, such states are sometimes distinguished by the term Hard Snowball. States in which sea ice and active land ice sheets reach the tropics but in which substantial areas of open tropical ocean remain are sometimes termed Soft Snowballs or Slushballs. These terms are inappropriate, however, because there is really no "slush" involved in these states. Instead, we refer to them as Waterbelt states.

The basic physical concepts governing transitions into and out of a Snowball or Waterbelt state are introduced in Section 3. The main issues include the following: the conditions for entry into a Snowball or Waterbelt state (Section 4), the nature of the climate during a Snowball state (Section 5), the conditions for deglaciation from a Snowball state (Section 6), and the nature of the climate following deglaciation (Section 7). We attempt to put these matters in context within the bigger picture of biogeochemical fluctuations within the Neoproterozoic, particularly regarding

the carbon cycle, the stages of oxygenation of the atmosphere and ocean, and the associated changes in the greenhouse gas inventory of the atmosphere.

Although this review is concerned with the events of the Neoproterozoic as they played out on Earth, the Snowball glaciations and associated carbon cycle fluctuations represent a generic habitability crisis for planets with substantial oceans. These phenomena greatly affect the prospects for occurrence of habitable extrasolar planets and also provide an essential part of the framework for interpretation of the rapidly growing inventory of extrasolar planet observations.

2. THE NEOPROTEROZOIC WORLD

2.1. Physical Characteristics

Lunar tidal stresses cause Earth's rotation rate to decrease over time; the Neoproterozoic solar day is estimated to have been approximately 22 h long (Schmidt & Williams 1995). This leads to a modest increase in the Coriolis force and slight modifications in the diurnal cycle, but climate models indicate that these effects play a minor role in Neoproterozoic climate. Geodynamic models indicate that Earth's obliquity was almost certainly near its present value and that it fluctuated in a narrow range comparable with that seen over the more recent past (Levrard & Laskar 2003). Similarly, the maximum eccentricity visited by Earth's orbit over the past four billion years is not likely to have deviated much from its Pleistocene range (Laskar 1996).

Solar luminosity was approximately 94% of its present value at the beginning of the Neoproterozoic, increasing to 95% by the end of the period (Gough 1981). On the basis of a present solar constant of 1,367 W m^{-2} and a planetary albedo of 30%, the absorbed solar radiation averaged over Earth's surface would have been approximately 14 W m^{-2} less than it is at present. A typical climate sensitivity of 0.5 K/(W m^{-2}) yields a global mean cooling of 7 K—somewhat larger than the Pleistocene glacial/interglacial range. To keep the Neoproterozoic temperature the same as today, the CO_2 concentration would have to be increased to approximately 12 times the preindustrial value (i.e., to 3,360 ppmv), assuming that the cloud and water vapor radiative effect remain as they are today. Methane could have substituted for some of the required CO_2, as is discussed in Section 4.2.

Land plants did not emerge until long after the close of the Neoproterozoic. The absence of land plants would make silicate weathering less efficient (Berner 2004), although it is reasonable to speculate that microbial ecosystems existed on land and that they might have enhanced silicate weathering relative to a completely abiotic land surface. All other things being equal, one would thus expect the Neoproterozoic, and the early Phanerozoic as well, to be warmer than the typical climates following the colonization of land by plants in the Ordovician (450 Mya). The typical nonglacial Neoproterozoic CO_2 would probably be in excess of the 3,360 ppmv that would maintain the partially glaciated climate of the present. The absence of land plants also affects the albedo, roughness, and hydrological properties of land surfaces employed in Neoproterozoic climate models.

The Neoproterozoic is punctuated by two great glaciations—the Sturtian at 720 Mya and the Marinoan at 635 Mya—which constitute the most dramatic and charismatic events of the Neoproterozoic, apart from the appearance of metazoan life toward the end of the period. These are no ordinary glaciations, such as those from the Pleistocene. Paleomagnetic data show that the Sturtian and Marinoan glaciations involve active land ice sheets discharging into the ocean near the equator. Evidence for tropical glaciation includes dropstones, striations, and characteristic sedimentary deposits known as diamictites. There is an additional well-documented glaciation—the Gaskiers at approximately 580 Mya—but this event does not have features that distinguish it

Luminosity: the net energy output of a star, per unit time

Solar constant: the flux of energy from the Sun, measured at the mean orbit of Earth

ppmv: parts per million by count of molecules; equal to molar concentration measured in parts per million

Dropstones: rocks transported into open water by ice and dropped into sedimentary layers

Striations: scratches in rocks likely caused by a glacier dragging small, hard debris over their surfaces

Diamictites: sedimentary deposits made up of components poorly sorted in size and often fairly large (generally interpreted as being of glacial origin)

from the general run of glaciations occurring later in Earth history. There is no known glaciation between the Makganyene Snowball glaciation at the beginning of the Proterozoic and the Sturtian, nearly a billion years later.

Makganyene: a Snowball-type glaciation that occurred near the beginning of the Paleoproterozoic, approximately 2.2 billion years ago

Because the glacial periods represent a hiatus in carbonate deposition, getting a precise estimate of the durations of the glaciations is difficult. Bodiselitsch et al. (2005) report large iridium anomalies in sediments of Marinoan age. Because iridium accumulates very slowly, the concentrated iridium anomalies imply accumulation on the ice surface of a globally glaciated world over a great period of time, followed by release into the sediments during deglaciation. Because the flow of sea ice in a partially glaciated state would carry most deposited iridium to the tropical water and dump it there gradually (see Section 5.3), the iridium anomaly appears most consistent with global glaciation of long duration. On the basis of likely accumulation rates, Bodiselitsch et al. (2005) estimate the Marinoan glaciation to have lasted at least three million years, with a probable duration of 12 million years. Before this interpretation can be considered secure, however, the iridium spike needs to be confirmed at other sites.

Neoproterozoic paleogeography has been discussed in Li et al. (2008) and Trindade & Macouin (2007). During the earliest part of the Neoproterozoic, the continents assembled into a tropical supercontinent known as Rodinia. The assembly was essentially complete by 900 Mya. By 725 Mya, Rodinia had centered itself near the equator and had begun to break up. The Sturtian glaciation occurred during the early stages of the breakup (**Figure 1**). The geography at the time of the Marinoan glaciation (**Figure 1**) represents a continuation of the breakup of Rodinia, with a drift of major land masses into the Southern Hemisphere. By 530 Mya, most of the continental area had reassembled into the supercontinent known as Gondwanaland, which extended from the South Pole into the tropics.

2.2. The Carbon Cycle

The stable isotopic composition of carbon preserved in the geological record provides a window into the operation of Earth's carbon cycle. Carbon has two stable isotopes, ^{12}C and ^{13}C; the first is by far the dominant in the Earth system. Carbon (mostly in the form of CO_2) is outgassed from the interior of Earth with a composition of $\delta^{13}C = -6‰$, and in a steady-state abiotic world in which all outgassing was balanced by reaction with silicate rocks to form carbonates, the carbonates would have the same isotopic composition. Deviation from equilibrium or separation of carbon into distinct reservoirs can lead to carbon isotopic excursions. Organic carbon produced by photosynthetic marine biota is shifted by $\sim -25‰$ relative to the carbon pool from which it is made. To the extent that some of the outgassed carbon is sequestered as light organic carbon, the carbonate deposits are shifted correspondingly toward positive values. Interpretation of the isotopic record is considerably more complicated when the carbon cycle is substantially out of equilibrium, because one then must consider interchanges of carbon among the many distinct reservoirs in which it may reside. Conventional thinking maintains that the organic carbon accumulates in marine sediments, but Rothman et al. (2003) hypothesized that in the Proterozoic a significant portion may reside in a dissolved or suspended organic carbon pool. Such a pool would be much more subject to oxidation than buried sedimentary organic carbon, if oxidants become available in sufficient quantities.

The Neoproterozoic is a time of extreme carbon isotopic excursions. **Figure 2** shows a long-term record of the variations of $\delta^{13}C$ in carbonate, with detailed high-resolution data for selected sections shown in the insets. Over the Proterozoic, the general pattern consists of a period of strong fluctuations at the dawn of the Proterozoic followed by a long period of stasis that terminates with resumption of massive fluctuations during the Neoproterozoic. After the Neoproterozoic, Earth

Figure 1

Marinoan and Sturtian paleogeography. Based on Li et al. (2008).

never again exhibits such large fluctuations in $\delta^{13}C$. There are long periods in which carbonate $\delta^{13}C$ is much more positive than values prevailing in the Phanerozoic—up to 8‰ in some cases. This value suggests a high proportion of organic carbon burial, although it does not in itself indicate high biological productivity. These periods are interrupted by major excursions that often take $\delta^{13}C$ to substantially negative values. The Sturtian and Marinoan glaciations are nestled amid

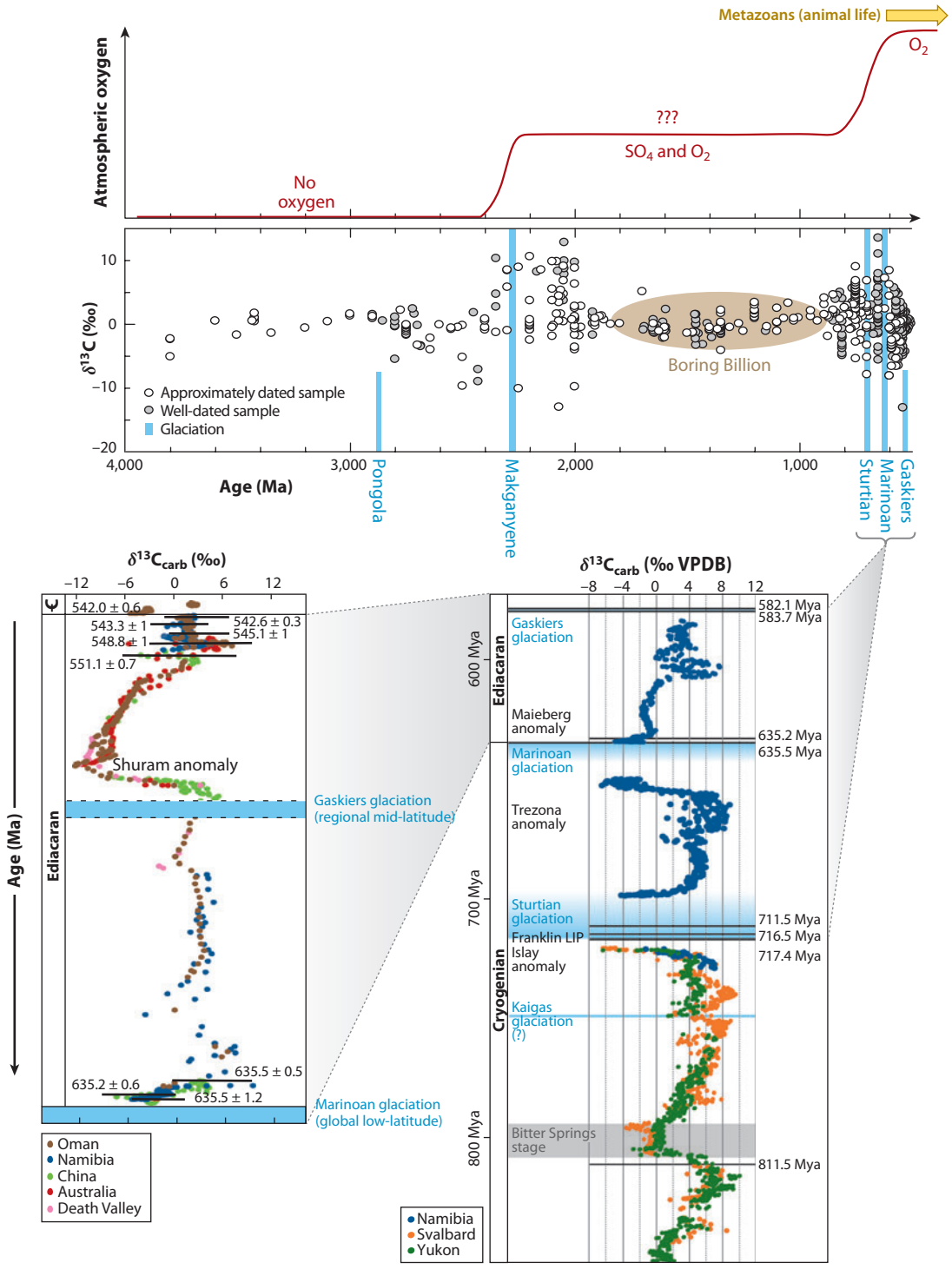

two of these negative excursions. The $\delta^{13}C$ goes negative before the glaciation and gradually recovers to positive values after deglaciation. The Shuram anomaly of the late Neoproterozoic is the greatest $\delta^{13}C$ fluctuation in Earth history, bottoming out at −12‰. In contrast to the Sturtian and Marinoan excursions, the Shuram anomaly does not have a glaciation nestled in its midst; in fact, it comes well after the relatively minor Gaskiers glaciation. This poses a great challenge for understanding Neoproterozoic carbon isotopic excursions. If all three major excursions arise from the same mechanism, how can the strongest of all fail to produce a glaciation?

The extreme negative values of $\delta^{13}C$ in the Shuram anomaly are problematic, because no mechanisms can drive them more negative than the mantle-outgassing value in equilibrium, and coming up with plausible mechanisms that work out of equilibrium is not easy, either. Arguing on the basis of the decorrelation of the $\delta^{13}C$ of organic carbon in the Shuram deposit from that of carbonate, Fike et al. (2006) proposed that the anomaly arises from the oxidation of the isotopically light organic carbon pool hypothesized by Rothman et al. (2003). Swanson-Hysell et al. (2010) have argued similarly for the pre-Marinoan excursion. An alternate possibility, however, is that the Shuram anomaly results from local rock-water interactions, as argued by Derry (2010), and that it is not indicative of changes in the global carbon cycle. Bristow & Kennedy (2008) point out that the interpretation of the Shuram anomaly as a global-scale organic carbon oxidation event is difficult to reconcile with the likely supply of oxidants.

Oxygenic photosynthesis intercepts volcanic CO_2 and allows some of the carbon to be buried as organic carbon rather than carbonate. This process turns CO_2, which is a greenhouse gas, into O_2, which is not, and would cause cooling if it happened too rapidly to be buffered by the silicate weathering thermostat. Conversely, oxidation of organic carbon would release CO_2 and lead to warming. Even if an organic carbon pool were not tapped, reduction in the rate of organic carbon burial would allow more volcanic CO_2 to accumulate in the atmosphere, leading to warming. Thus, if the organic carbon cycle is involved in Neoproterozoic negative ^{13}C excursions, accounting for the extreme cold needed to produce Sturtian and Marinoan glaciations becomes difficult. However, Swanson-Hysell et al. (2010) note that the negative carbonate ^{13}C excursion comes long before the Marinoan glaciation and that $\delta^{13}C$ recovers to zero by the beginning of the glaciation. This suggests that a warm phase is temporally separated from the glaciation and that the cooling may be associated with drawdown of CO_2 and restocking of organic carbon. This scenario still begs the question of how (and if) the negative excursions are related to subsequent glaciations, and why the excursion fails to produce a glaciation in the Shuram case.

The preglacial carbon isotopic excursions remain enigmatic, but the hypothesis of a globally glaciated Snowball state provides a consistent explanation for the negative postglacial $\delta^{13}C$. The general idea, proposed by Hoffman et al. (1998), is that photosynthesis largely shuts down when the ocean freezes over, so that the atmosphere-ocean carbon pool reverts to the abiotic mantle value over the millions of years of the glaciation. Because of the "stickiness" of the Snowball state, CO_2 must build up to very high values to trigger deglaciation (see Section 3). Results on

Figure 2

Summary of the Neoproterozoic carbon cycle as revealed by $\delta^{13}C$ in carbonates. The main frame is based on Hayes & Waldbauer (2006). Blue vertical bars on the main panel indicate glaciations, with short bars corresponding to nonglobal glaciations and long bars indicating Snowball glaciations, which involve low-latitude ice. A schematic history of atmospheric oxygen based on Canfield (2005) is sketched above the panel. Inset for the Shuram anomaly is based on Fike et al. (2006); inset for the Sturtian and Marinoan aged anomalies is based on Macdonald et al. (2009). Numbers annotating horizontal lines in the insets give the ages of dated layers, in Mya. Abbreviations: VPDB, Vienna PeeDee Belemnite (a geochemical standard for measuring carbon isotopes); LIP, Large Igneous Province (a geological formation indicative of massive volcanic activity, for example flood basalts).

oxygen mass-independent fractionation reported by Bao et al. (2009) are most readily interpreted as accumulation of very high levels of CO_2 prior to deglaciation and therefore support this picture. In the Marinoan event, for which high-resolution postglacial sections are available, the $\delta^{13}C$ starts at −3‰ following the glaciation and then drops to −5‰ before gradually recovering to positive values. The carbon cycle in the postglacial world is far out of equilibrium. The pattern of $\delta^{13}C$ laid down as the isotopically light atmosphere-ocean inorganic carbon pool is progressively transferred to carbonate is affected by Rayleigh distillation and by dissolution of land carbonates, as elucidated by Higgins & Schrag (2003).

Methane provides another lever affecting both climate (because it is a greenhouse gas) and carbon isotopic excursions. Methanogens metabolizing organic carbon produce methane with $\delta^{13}C \approx -60‰$. When the methane oxidizes to CO_2 in the atmosphere and ocean, it leads to a negative carbon isotopic excursion, but only if the reservoir of heavy carbon left behind by methanogenesis is kept from remixing with the new inorganic carbon being deposited. The only known way to achieve this is to stock methane in seafloor sediments in the form of hybrid methane/water ices known as clathrates, which later release methane through either catastrophic destabilization or a more gradual process. Jiang et al. (2003) have found evidence for methane seeps in arguably Marinoan-age cap carbonates from the Nantuo formation in South China. Kennedy et al. (2008) also found support for methane release around the time of the Marinoan deglaciation; they estimate that the release of 2,400 gigatonnes (Gt) of −60‰ carbon in the form of methane would lead to a −3‰ excursion in the carbonates.

Mass-independent fractionation: a form of isotopic separation that is only weakly dependent on molecular weight

Cap carbonates: carbonate deposits that indicate extreme carbonate supersaturation in the ocean and rapid deposition; the main indicator that the Neoproterozoic low-latitude glaciations and deglaciations involve a switch between extremely different states

Sulfur mass-independent fractionation: a form of isotope separation produced by photochemistry in the upper atmosphere and preserved in sediments only when atmospheric oxygen concentrations are extremely low

2.3. Oxygen

The oxygen story is woven throughout the Neoproterozoic. It is plausible that the emergence of metazoans at the end of the Neoproterozoic was enabled by an increase in oxygen to near-present levels. Methane connects with the oxygen story because the availability of oxidants in the atmosphere and ocean determines the rate at which methane is converted to CO_2. More generally, the $\delta^{13}C$ fluctuations connect to the oxygen story through the burial of organic carbon because accumulation of O_2 and other oxidants in the atmosphere-ocean system requires that organic carbon be sequestered where it cannot be immediately reoxidized. Unambiguous proxies of oxygen accumulation are not available for the Neoproterozoic, but mass-independent fractionation of sulfur decisively identifies a Great Oxidation Event at the beginning of the Proterozoic, and that period, too, exhibits large-amplitude $\delta^{13}C$ fluctuations (Canfield 2005). It is reasonable to assume by way of analogy that the $\delta^{13}C$ fluctuations of the Neoproterozoic also had something to do with adjustment of the carbon cycle to a more oxygenated world, especially in view of the fact that the analogy is strengthened by the occurrence of low-latitude glaciations in both the Neoproterozoic and Paleoproterozoic. Oxygen need not accumulate in the form of free O_2. Instead, it can accumulate in the oceans as sulfate (SO_4^{2-}), produced by oxidative weathering of pyrite (FeS_2) on land. Sulfate-reducing bacteria in the ocean can use sulfate to oxidize organic matter and liberate CO_2 and H_2S. If nutrients limit productivity of sulfate reducers, then an ocean can be anoxic but rich in both sulfate and organic carbon. Active sulfate reduction in an ocean, which can be detected through sulfur isotope fractionation, indicates the accumulation of an amount of oxygen in the atmosphere sufficient to permit oxidative weathering of pyrite.

The reappearance of banded iron formations (BIFs) in the Neoproterozoic, after a long absence, also indicates that something interesting was going on with oxygen during this time. Formation of BIFs requires that large amounts of soluble iron must first exist in the ocean, which can happen only if major portions of the ocean are anoxic. The reservoir also must be low in sulfate; if sulfate is present in considerable quantities, sulfate-reducing bacteria can use it as an oxidizing

agent, leading ultimately to the deposition of pyrite before the iron can be deposited as oxides in BIFs. The BIFs are deposited where iron-rich anoxic water comes into contact with oxygen. Neoproterozoic BIFs do not form in the aftermath of the major glaciations, as might be expected from a scenario in which the ocean reoxygenates upon deglaciation. Rather, they are interbedded with or below diamictites and sometimes exhibit glacial features such as dropstones. The way to fit this into the Snowball picture is to assume that the deep ocean is anoxic—and also low in sulfate because of the cessation of land weathering—but that limited coastal oases remain oxygenated; it is in these oases that the BIFs were presumably deposited. BIFs can also form without free O_2, via anoxygenic photosynthetic Fe^{++}-oxidizing bacteria (Kappler et al. 2005), as was clearly the case in the Archean. This mechanism still requires large parts of the ocean to be anoxic, so soluble iron can be mobilized, and still requires some open water or thin ice where the bacteria would get an adequate supply of light.

BIF: banded iron formation

Eukaryote: a cell with a complex, differentiated internal structure, including a nucleus containing genetic material

Doushantuo: a formation in China containing a wealth of well-preserved multicellular fossils

2.4. Life

Biomarker evidence shows that a flourishing and diverse microbial ecosystem, including complex eukaryotes, was already in place by the beginning of the Proterozoic (Waldbauer et al. 2009), although eukaryotic microfossils do not make their appearance until midway through the Proterozoic. The survival of these eukaryotes, particularly photosynthetic ones, poses a considerable challenge for the Snowball hypothesis. It has been conjectured that, in a Snowball, eukaryotes survive in small and perhaps intermittent open-water oases. If you are only a few microns in diameter, a pond can seem like a whole universe.

The frond-like Ediacaran biota appear at 575 Mya, roughly contemporaneous with the Shuram excursion and well after the Marinoan glaciation. The early metazoan embryos of the Doushantuo formation also date back to a time near the onset of the Shuram anomaly (Xiao & Knoll 2000). Mobile bilaterian animals, however, come in at 555 Mya, which is unambiguously at the close of the Shuram anomaly. Metazoans and multicellular plants require high levels of free oxygen to support their metabolism, so the rise of metazoans (especially mobile ones) in the late Neoproterozoic also suggests a rise in oxygen at the time. However, biomarkers suggest that sponges may have evolved before the Marinoan (Love et al. 2009). The survival of sponges, if confirmed, would present a greater challenge for the Snowball hypothesis.

2.5. Cap Carbonates

Sturtian and Marinoan glacial deposits occur as part of a characteristic carbonate sequence, which is striking in that carbonates rarely—if ever—occur in association with glacial deposits during the Phanerozoic. Right above (i.e., chronologically after) the Marinoan glacial diamictites, one finds a cap dolostone. Dolomite (magnesium carbonate) is believed to be deposited only under conditions of low sulfur availability, which provides a clue as to the state of the ocean. The cap dolostones often contain giant wave ripples. These features result from wave action on sediments in near-shore environments, and the physical understanding of the deposition process implies that the timescale of formation is quite short. Thus, the giant wave ripples show that the cap dolostone was precipitated rapidly. Other characteristic textures known as peloids also constitute a signature of rapid deposition. Above the cap dolostone, one sometimes finds limestone cements containing giant crystal structures known as aragonite fans. These are symptomatic of diffusion-limited crystal growth in situ in a highly supersaturated environment. As the crystals grow, they are buried by sedimentation of limestone from the water column, and this, too, suggests rapid deposition. Further up in the sequence, one finds either a thick limestone layer (as in Namibia)

or a thick layer of carbonate-poor shale. In toto, the structure is referred to as a cap carbonate sequence.

Deposits with the features of the cap dolostone and postglacial limestone cements are not seen during the Phanerozoic. All current interpretations of these enigmatic deposits require a mechanism that allows a rapid, massive increase in the carbonate ion content of the ocean waters. There is a need for something catastrophic, something with a switch that can cause an avalanche of carbonate into the ocean. The Snowball Earth scenario does have such a switch. As discussed in Sections 3 and 6, once global glaciation occurs, atmospheric CO_2 must build up to very high concentrations to make deglaciation possible, but once deglaciation starts, it proceeds rapidly. In fact, Kirschvink's (1992) proposal that deglaciation would occur through massive buildup of CO_2 after a glacial shutdown of silicate weathering revived the hypothesis of a truly global Snowball glaciation. Later, Hoffman et al. (1998) connected Kirschvink's scenario with the carbonate deposition and carbon isotope story.

In the Snowball scenario, cap dolostones are deposited when deglaciation leaves Earth in a hot, high CO_2 state. The resulting deluge of hot acid rain over exposed carbonate on land washes carbonate ion into the ocean, leading to supersaturation and precipitation. Cap dolostones are transgressive—that is, they are laid down as the sea invades inland progressively during a period of rapid sea-level rise following deglaciation (Hoffman et al. 2007). The rapid carbonate weathering continues for a time, leading to the deposition of limestone cements and aragonite fans. As sea level rises, however, exposed carbonate platforms are flooded and are no longer subject to weathering by rainfall. There follows a longer, more gradual period in which carbonate is generated on land by silicate weathering in a process that draws the atmospheric CO_2 back down to more moderate levels. The presence of magnetic reversals in some cap carbonates, however, poses a serious challenge to the otherwise compelling evidence that cap carbonate sequences were deposited rapidly (Trindade et al. 2003).

Pleistocene-type partial glaciations—even extreme versions with low-latitude sea-ice margins—do not have the kind of switch that the Snowball state exhibits because the ice-albedo feedback operates more continuously when there are major stretches of open water. As CO_2 increases, the sea-ice margin either melts back gradually or, at most, undergoes a deglaciation transition following a modest increase of CO_2. This situation offers no opportunity for CO_2 to build up to extreme levels and then avalanche carbonate into the ocean. A mechanism other than the Snowball might provide the required carbonate avalanche, perhaps through some switch in ocean circulation modes affecting the ocean stratification. At the time of writing, however, no such mechanism admitting of a sound physical quantification has been put forth. Shields (2005) put forth an interesting conjecture on the formation of cap carbonates without a Snowball episode, but extensive coupled geochemical/climate simulations would have to be carried out to test whether the idea is viable.

The cap carbonate sequences found after the Sturtian glaciation share some of the features of the Marinoan case but generally lack clear indications of rapid deposition. More information about the stratigraphic sequence and the differences between the Sturtian and Marinoan can be found in Hoffman & Schrag (2002), Shields (2005), and Pruss et al. (2010).

2.6. Neoproterozoic Weirdness: What Needs to Be Explained

Even more basic than the question of whether Earth experienced a Snowball state in the Neoproterozoic is the question of why glaciations resumed after a billion-year absence—and thereafter became quite common in the rest of Earth history. The reappearance of glaciations is an indication of some major reorganization of the biogeochemical cycle, involving carbon, oxygen, and possibly

methane and the sulfur cycle. Regardless of whether the Sturtian and Marinoan glaciations are Snowball events involving a globally frozen ocean, it is undeniable that these are extreme glacial events of a sort not seen later in Earth history—events involving low-latitude ice followed by a peculiar form of carbonate deposition. This demands an explanation. There is thus no shortage of Neoproterozoic weirdness that needs to be accounted for.

The similarities to the Paleoproterozoic with regard to ^{13}C, glaciation, and oxygenation are striking. Was the Makganyene event a trial run for planetary oxygenation? But why did the biogeochemical turbulence stop, only to resume a billion years later in the Neoproterozoic?

3. THE SNOWBALL BIFURCATION

Because ice and snow are so reflective, the solar luminosity and atmospheric composition conditions that can maintain a climate state with substantial areas of open water can also, under many circumstances, support an additional state in which the oceans are completely frozen over. The frozen ocean reflects enough sunlight to keep the planet frozen if it somehow gets into that state. Multiple equilibria are common in nonlinear systems, and when they exist, new equilibria can appear or disappear discontinuously as a control parameter (e.g., atmospheric CO_2) is varied continuously. The term bifurcation refers to the appearance and disappearance of states, and the disappearance of a state results in the system discontinuously switching to an alternate state as the control parameter is continuously varied. A related phenomenon is hysteresis, in which changing the control parameter and then returning it to its original value leaves the system in a state different from its original one. The Snowball bifurcation involves transitions between radically different states, and it is therefore natural to suppose that it plays a role in accounting for why the Neoproterozoic glacial/interglacial transitions are so different from the gentler ones that prevailed during the Phanerozoic. The Earth system admits of other bifurcations, including some that involve transitions between alternate states with substantial open water, but none that have come to light so far offer the same opportunities as does the Snowball bifurcation when it comes to accounting for Neoproterozoic weirdness.

3.1. Digression: Characterization of High CO_2 States

Deglaciation can involve very high CO_2 concentrations, so some attention must be paid to the way in which atmospheric composition is expressed. Approximations appropriate to the conventional low-concentration case break down because the mean molecular weight of the atmosphere changes significantly when large amounts of CO_2 are added. This breakdown can be a source of considerable confusion. To measure the CO_2 inventory of the atmosphere, we introduce the pressure p_{I,CO_2}, which is the surface pressure that the CO_2 in the atmosphere would have if it were the sole component of the atmosphere. From the hydrostatic relation, the mass of CO_2 in the atmosphere is $Ap_{I,CO_2}/g$, where A is the surface area of Earth and g is the acceleration of gravity; this quantity can be converted to moles through division by the molecular weight of CO_2. An inventory of 1 Pa corresponds to $1.18 \cdot 10^{15}$ mol or 14.16 Gt of total atmospheric carbon. The inventory of dry background air (mostly N_2 and O_2), termed $p_{I,a}$, is defined similarly. If water vapor is ignored for the moment, the total surface pressure is $p_{tot} = p_{I,CO_2} + p_{I,a}$. The molar concentration of CO_2, if it is well mixed, is then $(p_{I,CO_2}/m_{CO_2})/(p_{I,CO_2}/m_{CO_2} + p_{I,a}/m_a)$, where m_{CO_2} is the molecular weight of CO_2 and m_a is that of dry, non-CO_2 air. If χ is the molar concentration, then Dalton's law implies that the partial pressures of the two components are $p_{CO_2} = \chi p_{tot}$ and $p_a = (1 - \chi)p_{tot}$. The partial pressure of background air increases as more CO_2 is added to the atmosphere while $p_{I,a}$ is kept fixed. Some typical values are shown in **Table 1**. Except in the dilute limit, the CO_2

Table 1 Conversion between various characterizations of Earth's atmospheric CO_2 content

Total atmospheric CO_2 (10^{18} mol)	p_{I,CO_2}[a] (Pa)	p_{CO_2}[b] (Pa)	p_a[c] (Pa)	p_{tot} (Pa)	Molar concentration[d] (ppmv)
0.0118	10	6.6	$1.000 \cdot 10^5$	$1.000 \cdot 10^5$	66.0
0.118	100	66.0	$1.000 \cdot 10^5$	$1.001 \cdot 10^5$	658.7
1.18	1000	661.3	$1.003 \cdot 10^5$	$1.001 \cdot 10^5$	6547.7
11.8	10^4	6801.	$1.032 \cdot 10^5$	$1.1 \cdot 10^5$	$6.18 \cdot 10^4$
118.	10^5	$7.95 \cdot 10^4$	$1.21 \cdot 10^5$	$2.00 \cdot 10^5$	$39.7 \cdot 10^4$
1180.	10^6	$9.55 \cdot 10^5$	$1.45 \cdot 10^5$	$1.1 \cdot 10^6$	$86.8 \cdot 10^4$

[a] p_{I,CO_2} is the surface pressure the CO_2 would exert if it were unmixed with any other gases.
[b] p_{CO_2} is the partial pressure of CO_2 when it is mixed with the background air. Results were computed for $p_{I,a} = 10^5$ Pa (10^5 Pa = 1 bar = 1,000 mbar).
[c] p_a is the resulting partial pressure of air in the mixture.
[d] The final column gives the molar concentration of CO_2, which is nearly the same as the volumetric mixing ratio for small concentrations. 10^4 ppmv = 1%.

molar concentration is not linear in the CO_2 inventory. For example, the CO_2 inventory has to be increased by a factor of 10 to increase the molar concentration from 6.18% to 39.7%. Also, the partial pressure of CO_2 when it is mixed into the atmosphere is below p_{I,CO_2} by a factor of $\frac{29}{44}$ when the CO_2 is a minor constituent but asymptotes to p_{I,CO_2} when CO_2 becomes the dominant component of the atmosphere.

When the CO_2 inventory becomes high, the increase of total surface pressure increases the infrared opacity of all the greenhouse gases in the atmosphere, including water vapor. This occurs because the more frequent collisions that go along with high pressure broaden spectral lines and allow the gases to absorb over a broader range of the spectrum. This effect becomes important as the molar concentration is increased beyond 20%. The warming effect of pressure broadening is offset partly by increased Rayleigh scattering as the mass of the atmosphere increases, but for a Snowball state with a highly reflective surface, the resulting increase in planetary albedo is not significant. The radiation calculations used in this section incorporate the effect of pressure broadening, but we have not taken into account the additional Rayleigh scattering in the computation of the albedo. If Neoproterozoic oxygen concentrations were substantially below modern values, this would bring down the surface pressure and reduce the pressure broadening. For example, reducing the atmospheric O_2 inventory to 10% of its current value would reduce the surface pressure from approximately 10^5 Pa to $0.8 \cdot 10^5$ Pa. Water vapor also affects the surface pressure and the mean molecular weight of the atmosphere, but the water vapor content of the atmosphere is low in the cold conditions that prevailed during initiation of a Snowball event and in the Snowball state itself. During the postglacial hothouse, however, the effect of water vapor on surface pressure and mean molecular weight becomes significant.

3.2. A Zero-Dimensional Model of the Snowball Bifurcation

Zero-dimensional model: model in which the entire climate is represented by a single mean temperature

The Snowball bifurcation was discovered by Budyko (1969) and Sellers (1969), although it was considered a mathematical curiosity until Kirschvink (1992) provided an exit strategy and techniques for analysis of the geological record caught up with the imaginations of mathematicians. The essential features of the Snowball bifurcation and consequent hysteresis are well illustrated even in the simplest zero-dimensional form of energy balance model (EBM). In such models, the entire climate is represented by a single global mean surface temperature T. The albedo α is written as a function of T. Here we assume that T represents an annual average temperature, which

can be taken to be time independent. All information about dynamical heat transports, the meridional temperature gradient, and the physics of ice formation enter the problem only through the functional form of $\alpha(T)$. Earth is assumed to be globally ice covered for $T < T_i$, with an albedo α_i. It is assumed to be ice free for $T > T_O$, with an albedo α_O that incorporates the reflectivity of clouds as well as ocean water and continents. At intermediate temperatures, the planet is partially ice covered, and we interpolate the albedo between extremes according to the formula

$$\alpha(T) = \begin{cases} \alpha_i & \text{for } T \le T_i, \\ \alpha_O + (\alpha_i - \alpha_O)\dfrac{(T - T_O)^2}{(T_i - T_O)^2} & \text{for } T_i < T < T_O\,. \\ \alpha_O & \text{for } T \ge T_O \end{cases} \quad (1)$$

The difference between T_i and T_O is a measure of the meridional temperature gradient and hence the efficiency of lateral heat transports. If the heat transports are strong enough to keep the planet nearly isothermal, then $T_i \approx T_O \approx T_f$, where T_f is the freezing temperature of seawater. Because the energy budget in calculations of this sort is done at the top of the atmosphere, the albedos should be interpreted as top-of-atmosphere albedos that incorporate the effects of Rayleigh scattering, clouds, and atmospheric solar absorption as well as the reflective properties of the surface.

To complete the model, we balance the absorption of solar radiation against the heat loss by infrared emission to space (termed OLR for outgoing longwave radiation). In simplified EBMs, the *OLR* value is written as a function of surface temperature through the introduction of assumptions about the vertical profiles of temperature and humidity. As in chapter 4 of Pierrehumbert (2010), we assume that the vertical profile is dictated by the moist adiabat and that relative humidity is constant up to the tropopause, with the stratosphere assumed isothermal and the stratospheric water vapor mixing ratio held fixed at the tropopause value. With these assumptions, the clear-sky *OLR*, termed OLR_{clr}, can be computed using an atmospheric radiation model; calculations here were carried out using the National Center for Atmospheric Research Community Climate Model (NCAR CCM) radiation model (Kiehl & Briegleb 1992, Kiehl et al. 1998), as described in chapter 4 of Pierrehumbert (2010) (see sidebar, The NCAR Radiation Code). The resulting function can be represented easily by a low-order polynomial fit, obviating the need to run the radiation model once the fitting coefficients are obtained. To keep things simple, we approximate cloud effects by subtracting a fixed increment Δ_{cld} from the clear-sky value, so that $OLR(T) = OLR_{clr}(T) - \Delta_{cld}$. For zero-dimensional models, the global mean surface temperature is used in the resulting $OLR(T)$, but in geographically resolved EBMs, one would use the local surface temperature instead.

The OLR is also a function of atmospheric composition, notably the CO_2 content of the atmosphere. With this in mind, the equation defining the global energy balance is

$$(1 - \alpha(T))\frac{L}{4} = OLR(T, p_{I,CO_2}), \quad (2)$$

Outgoing longwave (i.e., infrared) radiation (OLR): the rate at which a planet cools to space by emission of infrared radiation, usually expressed per unit surface area of the planet

THE NCAR RADIATION CODE

The National Center for Atmospheric Research (NCAR) radiation code is valid only for CO_2 inventories under 200 mbar. We have found through comparisons with comprehensive planetary codes, however, that when pressure broadening is included, the *OLR* calculated by the model remains accurate at least up to inventories of one bar because the *OLR* is dominated by the upper part of the atmosphere. The code cannot be used in general circulation model (GCM) integrations at such high inventories, however, because the low-level radiation fluxes become inaccurate owing to problems arising from the parameterization of overlap with water vapor absorption bands.

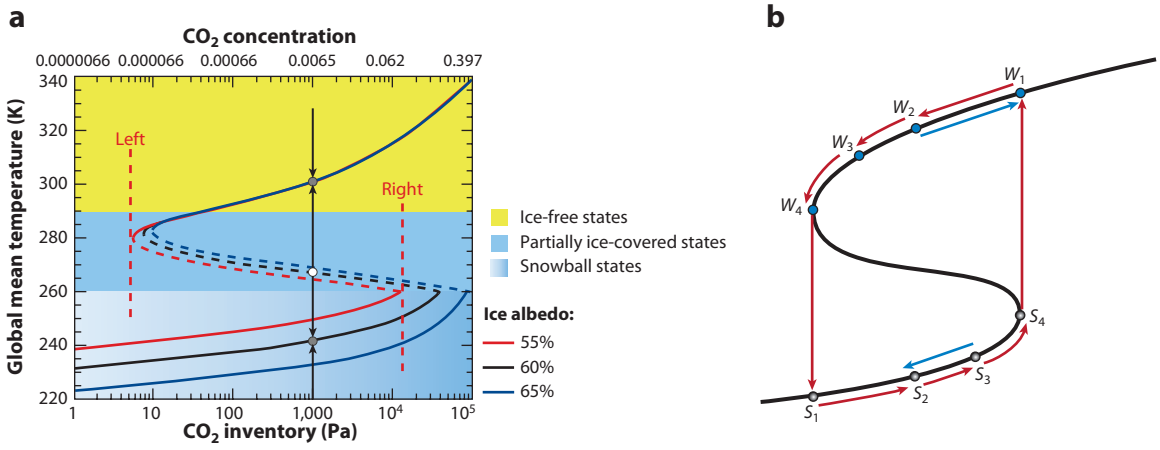

Figure 3

(*a*) Bifurcation diagram for the zero-dimensional energy balance model. Calculations performed with $L = 1{,}285$ W m^{-2}, $\alpha_O = 0.2$, $T_i = 260$ K, $T_O = 290$ K, $\Delta_{cld} = 20$ W m^{-2}, $p_{I,a} = 10^5$ Pa, and the three values of ice albedo indicated in the key. For CO_2 inventories up to approximately 1,000 Pa, the inventory can be converted to a mixing ratio in parts per million by volume (ppmv) by multiplying by 6.6. The CO_2 concentrations on the upper horizontal axis are stated as fractions (e.g., 0.0065 corresponds to 6,500 ppmv). The vertical dashed lines marked "Left" and "Right" indicate the left and right boundaries of the hysteresis loop for the case with ice albedo equal to 55%. (*b*) Illustration of the hysteresis phenomenon. W_1–W_4 indicate a sequence of warm states, whereas S_1–S_4 indicate a sequence of Snowball states.

where L is the value of the solar constant at Earth's orbit, at the time under consideration. Equation 2 defines a nonlinear equation for T given p_{I,CO_2}. Because it is nonlinear, it can, and generally does, have multiple solutions for a given set of parameters. The easiest way to find the full solution space is to pick a temperature T, evaluate the left side of Equation 2, and then adjust the p_{I,CO_2} until the *OLR* function takes on the value that balances the right side. This is easy to do, and it generally yields a unique solution $p_{I,CO_2}(T)$ because the *OLR* is almost invariably a monotonically decreasing function of p_{I,CO_2} for fixed T. To get the bifurcation diagram in the customary form, we then simply plot p_{I,CO_2} with temperature on the vertical axis. Results calculated with a Neoproterozoic value of the solar constant are shown for three values of ice albedo in **Figure 3**. An implementation of this model in the computer language Python is provided in the online Supplemental Material (follow the Supplemental Materials link from the Annual Reviews home page at **http://www.annualreviews.org**).

Supplemental Material

When p_{I,CO_2} is very small, there is only a single solution, which is a Snowball state; when p_{I,CO_2} is very large, there is again only a single solution, which, in this case, is an ice-free hothouse state. In between, there are three solutions, as indicated by circles for $p_{I,1CO_2} = 1{,}000$ Pa. The intermediate-temperature solution is unstable and separates the attractor basin of the upper warm state from the lower Snowball state. If the system starts in the warm state W_1 on the upper branch, it will evolve into the cooler state W_2 if the CO_2 is decreased but will return to W_1 if the CO_2 is returned to its original value. However, if the CO_2 is reduced so much that the system moves to state W_4, a slight further reduction will cause the system to fall into state S_1 on the Snowball branch, and returning the CO_2 to the value that originally supported state W_2 leaves the system in state S_2 rather than returning it to the upper branch. If the CO_2 is gradually increased further, the system will evolve into the Snowball state S_4, but a slight further increase will result in a discontinuous transition to the very warm upper-branch state W_1. This is an example of a hysteresis loop. The left and right limits of the hysteresis loop (see **Figure 3**) are the key features that determine the

conditions for entering and leaving a Snowball state. They can be evaluated in a hierarchy of models, from the simplest illustrated here to the most comprehensive atmosphere-ocean general circulation model (GCM).

The "stickiness" of the Snowball state—a feature that carries over to comprehensive GCMs—is what makes it attractive as an explanation for the unusual features of the Neoproterozoic.

GCM: general circulation model

One-dimensional model: a model in which temperature is a function of latitude

The results shown in **Figure 3** highlight the extreme sensitivity of the initiation and deglaciation thresholds to albedo. This is an inevitable consequence of the approximately logarithmic dependency of *OLR* on the CO_2 inventory. A small change of albedo, such as one that might be caused by differences in cloud or snow cover assumptions, requires a very large change of CO_2 to make up for it. Although the radiation balance cares only about the log of the CO_2 inventory, the large corresponding changes in the CO_2 itself have enormous implications for geochemistry and the prospects for getting out of a snowball by accumulation of CO_2. The same remark applies to the effect of clouds on *OLR*. For the value $\Delta_{cld} = 20$ W m^{-2} used in **Figure 3**, initiation occurs at $p_{I,CO_2} = 7.7$ Pa, and deglaciation occurs at $3.8 \cdot 10^4$ Pa. When $\Delta_{cld} = 0$, the values increase to 205 Pa for initiation and 10^5 Pa for deglaciation. The threshold for initiation is also sensitive to the choice of T_O, the threshold global mean temperature for ice-free conditions.

3.3. A One-Dimensional Model of the Snowball Bifurcation

The one-dimensional, steady, diffusive EBM is a useful extension of the zero-dimensional model. It rests on the assumption that the meridional atmosphere-ocean heat flux can be represented as proportional to the surface temperature gradient, leading to the diffusion equation

$$\frac{d}{dy} D \frac{d}{dy} T = (1 - \alpha(y, y_i)) L f(y) - OLR(T, p_{I,CO_2}), \quad (3)$$

where $y = \sin\phi$ and ϕ is latitude. The flux factor f describes the annual mean distribution of incident solar radiation over the surface; it satisfies $\int f dy = 1/4$. D is diffusivity, measured in W m^{-2} K^{-1}; the unconventional units arise because y is dimensionless. The albedo depends on y through the ice cover, characterized by the ice margin y_i. Typically α is set to α_i for $|y| > y_i$ and to α_O otherwise. Self-consistent solutions are found by varying y_i until the ice-margin temperature yielded by solving the diffusion equation equals the freezing point of seawater (or sometimes a value somewhat below that, to account for seasonality). The Snowball state corresponds to $y_i = 0$, in which case the ice can be arbitrarily cold because there is no open water to freeze. The Snowball bifurcation study of Caldeira & Kasting (1992) was a solution to a problem of this general type, based on approximate solutions to the diffusion equation obtained from a highly truncated Legendre polynomial expansion of $T(y)$.

Some results from the diffusive model are shown in **Table 2**. The observed meridional energy flux in the present climate implies $D \approx 0.5$ W m^{-2} K^{-1} (Pierrehumbert 2010, chapter 9), but in a cold Snowball climate, the lack of latent heat transport may reduce the heat transport efficiency considerably; hence we also show results for $D = 0.25$ W m^{-2} K^{-1}. These results confirm and strengthen the impression that it is hard to deglaciate a Snowball by elevated CO_2 alone. The minimum CO_2 inventory for deglaciation seen in any of the cases is 290 mbar (corresponding to $p_{CO_2} = 207$ mbar or a mole fraction of 16%). Even that requires the assistance of 30 W m^{-2} of cloud forcing and an assumption of very weak atmospheric heat transport. Moreover, high-albedo snow cover would raise the albedo above the value of 0.6 assumed in these calculations, making deglaciation even harder. Pressure broadening, however, makes the greenhouse effect increase faster than logarithmically with concentration at very high CO_2 inventories, so if one is at liberty to increase p_{I,CO_2} to a bar or more, it is possible to deglaciate even the more difficult cases.

Table 2 Initiation and deglaciation thresholds[a] for the one-dimensional diffusive energy balance model, for various values of diffusivity D and cloud longwave forcing Δ_{cld}

D (W m^{-2} K^{-1})	Δ_{cld} (W m^{-2})	p_{I,CO_2}, initiation (Pa)	ϕ_{min}[b] (°)	p_{I,CO_2}, deglaciation (Pa)
0.25	10	129	26°	$7.4 \cdot 10^4$
0.25	20	19	25°	$5.0 \cdot 10^4$
0.25	30	2	25°	$2.9 \cdot 10^4$
0.5	10	201	38°	$9.0 \cdot 10^4$
0.5	20	35	30°	$6.0 \cdot 10^4$
0.5	30	4.5	30°	$3.8 \cdot 10^4$

[a]All calculations were done with $\alpha_i = 0.6$ and $\alpha_O = 0.2$.

[b]ϕ_{min} is the limiting latitude: the minimum stable ice margin encountered before the system falls into a Snowball state.

[The logarithmic extrapolation to very high CO_2 mentioned briefly in Pierrehumbert (2004) did not take pressure broadening into account and therefore was overly pessimistic with regard to the prospects for deglaciation at CO_2 concentrations beyond the values treated explicitly in that study.] Such extreme concentrations are not relevant to the Neoproterozoic but could conceivably be of interest for the earlier Earth or for other planets.

The diffusive EBM results also indicate that the CO_2 concentration must fall to very low values in order to drive the planet into a Snowball, although in this case the albedo of snow cover would help rather than hinder the process. As the CO_2 approaches the initiation threshold from above, the ice margin moves toward the equator and reaches a minimum limiting latitude, at which point the tropics freeze over completely. The limiting latitude, which defines the minimum width of stable tropical open water in a Waterbelt state, is also given in **Table 2**. For an ice albedo of 0.6, it lies between 25° and 38°, depending on the diffusivity and cloud forcing. If the contrast between ice and ocean albedo is increased sufficiently, however, the stable states with partial ice cover disappear. For example, in the case with a cloud longwave forcing of 10 W m^{-2} and a diffusivity of 0.5 W m^{-2} K^{-1}, increasing the ice albedo to 0.65 is sufficient to eliminate the stable states with partial ice cover. When the contrast between ice and ocean albedo is high, the ice-albedo feedback is so strong that any ice formation destabilizes the system and causes the Snowball bifurcation. Conversely, low ice albedo stabilizes a low-latitude ice margin because low-albedo ice melts easily when it penetrates into the region of high tropical insolation. For the simpler Budyko model, similar results can be obtained analytically, using the formulas given in Roe & Baker (2010).

3.4. Snowball and Waterbelt States in Other Energy Balance Models

Stable Waterbelt states with low-latitude ice margins can exist, but because an increase in CO_2 causes effective warming of the adjacent dark ocean, it takes only a modest rise in CO_2 to cause such states to deglaciate (Crowley et al. 2001). In some models, such as the diffusive EBM discussed above, the ice line retreats continuously to the pole as the planet is made warmer. Given a sufficiently complex model, there can be additional folds in the bifurcation diagram, in which case the Waterbelt state undergoes a discontinuous transition to a state with reduced (but perhaps nonzero) ice coverage. Because of the narrow range of CO_2 over which Waterbelt climate transitions operate, it is difficult to reconcile them with the long-lived glaciated states and dramatic Earth system transitions that seem to be required by the geological record.

EBMs have been further elaborated to incorporate the seasonal cycle, two-dimensional geographical variations, and even some aspects of ocean dynamics (Crowley & Baum 1993, Donnadieu

et al. 2004, Lewis et al. 2003). They are valuable exploratory tools that can help make sense of the behavior of GCMs. However, the answer one obtains from EBMs is sensitive to the settings of various parameters that are difficult or impossible to determine a priori. Notably, albedo is determined largely by snow cover, but EBMs cannot predict this because they cannot represent the hydrological cycle adequately. Determination of heat transport and its variations with static stability and atmospheric moisture content, of cloud effects, and of the vertical structure of the atmosphere (which governs the greenhouse effect) are problematic. For further enlightenment, we thus turn to GCMs. GCMs also are subject to physical uncertainties, but they have the virtue that the assumptions one needs to make at least lie closer to the fundamental underlying physics.

Snowball model intercomparison (SNOWMIP) project: a protocol for GCM experiments on initiation and deglaciation of Snowball states

CAM: National Center for Atmospheric Research's Community Atmosphere Model v3.1

FOAM: Fast Ocean Atmosphere Model v1.5

ECHAM5: Max Planck Institute's atmospheric model v5.3.02p

4. INITIATION OF SNOWBALL STATES

The simplest EBMs indicate that the Snowball state is a stable state with a finite attractor basin. In fact, a stable Snowball state exists even with modern CO_2 and a present-day value of the solar constant; GCMs confirm that this is so (Marotzke & Botzet 2007, Voigt & Marotzke 2010). Thus, without change of CO_2 or absorbed solar radiation, a Snowball could be initiated if some transient event caused the ice margin to advance into the attractor basin of the Snowball state. It is hard to think of a plausible mechanism that could do a job this big, however. Usually, when one thinks of the Snowball initiation problem, one considers *forcing* the system to fall into a Snowball by changing the controlling parameters of the climate in such a way as to eliminate all stable non-Snowball states. Although the system could theoretically be forced into a Snowball state through suitable fluctuations in atmosphere-ocean heat transports, albedo, or solar luminosity, no plausible mechanisms employing any of these means have come forth. Attention to the initiation problem has centered on mechanisms that could reduce the greenhouse gas content of the atmosphere, primarily through drawdown of CO_2 or methane.

4.1. Threshold CO_2 for Initiation

In this section, we study Snowball initiation in global climate models, which calculate three-dimensional heat transports dynamically by solving the equations of motion. We focus in particular on the threshold CO_2 for initiating a Snowball. By threshold CO_2 for initiation, we mean the maximum CO_2 level at which a model enters a Snowball when started from ice-free conditions. In the consideration of mechanisms for Snowball initiation other than reduction in CO_2, such as reduction in methane (see Section 4.2), the threshold CO_2 discussed in this section should be viewed as a threshold in equivalent CO_2 radiative forcing.

Most of the results we present in this section were obtained from a variety of global climate models run in a consistent and simplified modeling framework to facilitate model intercomparison. We refer to this modeling framework as SNOWMIP, for Snowball model intercomparison. Three models participated in SNOWMIP: (*a*) the National Center for Atmospheric Research's Community Atmosphere Model v3.1 (CAM) (Collins et al. 2004, McCaa et al. 2004) run at T42 horizontal resolution with 26 vertical levels, (*b*) the Fast Ocean Atmosphere Model v1.5 (FOAM) (Jacob 1997) run at R15 horizontal resolution with 18 vertical levels, and (*c*) and the Max Planck Institute's atmospheric model v5.3.02p (ECHAM5) (Roeckner et al. 2003) run at T31 horizontal resolution with 19 vertical levels. Additionally, we present results from ECHAM5 coupled to the Max Planck Institute Ocean Model v.1.2.3p2 (Marsland et al. 2003) run with a nonuniform 114 × 106 horizontal grid and 39 unevenly spaced vertical levels (we refer to this fully coupled

model as ECHAM5/MPI-OM). The ECHAM5/MPI-OM runs were performed with realistic Neoproterozoic boundary conditions and are described in full by Voigt et al. (2010).

ECHAM5/MPI-OM: ECHAM5 coupled to the Max Planck Institute Ocean Model v.1.2.3p2

SNOWMIP is designed to isolate the effects that atmospheric dynamics, cloud schemes, and ice and snow albedo parameterizations have on Snowball initiation. For SNOWMIP, we ran various climate models in Aquaplanet mode (with only ocean at the surface). We used a mixed-layer ocean with a depth of 50 m to provide a reasonable simulation of the seasonal cycle, and we set ocean heat transport to zero everywhere. To ensure that the models were started within the zone of attraction of a warm climate state, if one exists, we started each model run with the sea-surface temperature set to 300 K globally. We set the solar constant to 1,285 W m^{-2}, 94% of its present value. For simplicity, we used circular orbits (an eccentricity of zero) and an obliquity of 23.5°. We ran the models with a rotation rate corresponding to a modern 24-h day. The main reason for this is that changing the length of day in many global climate models is difficult. Tests with the length of day reduced to its Neoproterozoic value of 22 h suggest that approximating the length of day as 24 h has a minor effect in comparison with the effects of the differences in albedo and cloud parameterizations that we consider here.

The SNOWMIP simulations differ slightly among models in their specifications of ozone, aerosols, and non-CO_2 greenhouse gases. In CAM, modern ozone levels were specified, all aerosols were set to zero, and modern values were used for non-CO_2 greenhouse gases ($CH_4 = 1.714 \cdot 10^{-6}$, $N_2O = 0.311 \cdot 10^{-6}$, $CFC_{11} = 0.280 \cdot 10^{-9}$, $CFC_{12} = 0.503 \cdot 10^{-9}$). In FOAM, symmetric (across the equator) ozone profiles based on modern ozone were specified, a small background aerosol that models modern aerosols simplistically was used, and all non-CO_2 greenhouse gases were set to zero. In ECHAM5, ozone profiles were specified as they were in FOAM, aerosols were set to zero, and all non-CO_2 greenhouse gases were set to zero. The radiative forcing associated with modern aerosol and non-CO_2 greenhouse gases is well below the forcing associated with a doubling of CO_2 (Solomon 2007).

We ran the models with three different ice and snow albedo parameterizations. In the first, which we term default albedos (**Figure 4*a***), we used the default model albedo parameterizations. In the second, which we term SNOWMIP albedos (**Figure 4*b***), we set the sea-ice albedo to 0.6 for all wavelengths and the snow albedo to 0.9 for all wavelengths, and we removed all temperature and ice-thickness albedo dependencies. In the third, which we term constant albedos (**Figure 4*c***), we set both the sea-ice and snow albedos to 0.6 for all wavelengths and removed all temperature and ice-thickness albedo dependencies. A summary of the salient features of the models' albedo parameterizations is presented in **Table 3**. ECHAM5 does not include snow over sea ice. Hence the albedo in ECHAM5 over sea ice is determined exclusively by the sea-ice albedo.

CAM forms two strange near-Snowball states when run with default albedos. In these states, the global sea-ice fraction reaches more than 80% in two cases. If we classify the near-Snowball states as Snowball states, both CAM and FOAM have a threshold CO_2 for initiation between 2,500 and 3,000 ppmv with default albedos (**Figure 4*a***). If we do not consider the near-Snowball states as Snowball states, the threshold CO_2 for initiation in CAM is between 1,000 and 2,000 ppmv. The similarity between the initiation thresholds in CAM and FOAM is reasonable because most of the sea ice is covered with cold snow during the initiation, and the models have similar cold snow albedos (**Table 3**). Furthermore, the similarity between CAM and FOAM implies that differences in other processes such as clouds do not cause the initiation threshold to diverge significantly between CAM and FOAM. This is consistent with the fact that the initiation threshold is the same in CAM and FOAM for SNOWMIP albedos (**Figure 4*b***), in which case only cloud and circulation differences could cause different model behavior. For default albedos, both CAM and FOAM produce fluctuating sea ice that covers less than 1% of the globe at $CO_2 = 3{,}000$ ppmv, whereas for SNOWMIP albedos, both initiate a Snowball at $CO_2 = 3{,}000$ ppmv. This indicates

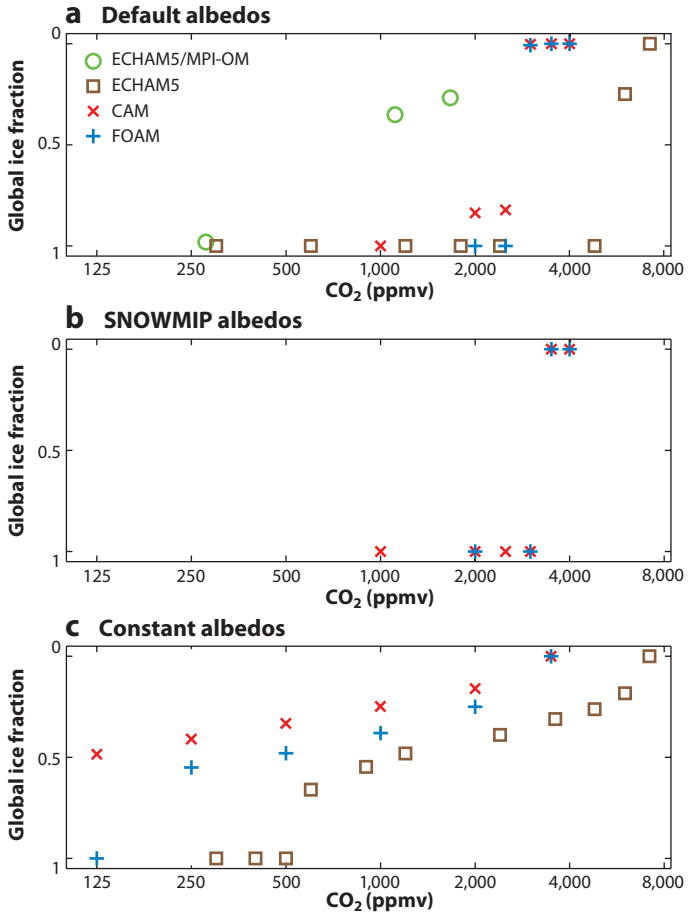

Figure 4

The equilibrated sea-ice fraction as a function of CO_2 for the Snowball model intercomparison (SNOWMIP) model runs in each albedo case: (*a*) default albedos, (*b*) SNOWMIP albedos, and (*c*) constant albedos. In the SNOWMIP albedo case, the sea-ice albedo is 0.6 and the snow albedo is 0.9. In the constant-albedo case, both the sea-ice and snow albedos are 0.6. Abbreviations: CAM, National Center for Atmospheric Research's Community Atmosphere Model v3.1; ECHAM5, Max Planck Institute's atmospheric model v5.3.02p; ECHAM5/MPI-OM, ECHAM5 coupled to the Max Planck Institute Ocean Model v.1.2.3p2; FOAM, Fast Ocean Atmosphere Model v1.5.

that CAM and FOAM enter a Snowball if even a tiny amount of ice forms for SNOWMIP albedos and that no states with intermediate ice cover are possible in CAM and FOAM with SNOWMIP albedos.

ECHAM5 has a threshold CO_2 for initiation between 4,800 and 6,000 ppmv when run with default albedos (**Figure 4*a***), which is roughly one doubling of CO_2 higher than the threshold CO_2 for initiation of CAM or FOAM. Snowball initiation is thus somewhat easier in ECHAM5 than it is in CAM and FOAM. This difference is interesting, given that the cold sea-ice albedo in ECHAM5 is similar to the cold snow albedo in CAM and FOAM (see **Table 3**; recall that ECHAM5 does not include snow cover over sea ice). The fact that ECHAM5 has a higher threshold CO_2 for initiation in SNOWMIP than does CAM and FOAM, therefore, is probably caused by different

Table 3 Summary of albedo parameterizations for models participating in SNOWMIP[a]

	CAM	FOAM	ECHAM5/ MPI-OM	ECHAM5	SNOWMIP[f]
Cold sea-ice albedo[b]	0.45	0.55	0.75	0.75	0.6
Warm sea-ice albedo[c]	0.38	0.50	0.55	0.55	0.6
Cold snow albedo[b]	0.79	0.72	0.8	–	0.9
Warm snow albedo[c]	0.66	0.43	0.65	–	0.9
Cold albedo temperature[d]	−1°C	−10°C	−1°C	−1°C	–
Albedo thickness scale[e]	1 m	1 m	–	–	–
Snow thickness scale[e]	∼0.05 m	∼0.05 m	0.01 m	–	–

[a]Abbreviations: CAM, National Center for Atmospheric Research's Community Atmosphere Model v3.1; ECHAM5, Max Planck Institute's atmospheric model v5.3.02p; ECHAM5/MPI-OM, ECHAM5 coupled to the Max Planck Institute Ocean Model v.1.2.3p2; FOAM, Fast Ocean Atmosphere Model v1.5; SNOWMIP, Snowball model intercomparison.
[b]The cold sea-ice or snow albedo is the albedo for temperatures at and below the cold albedo temperature.
[c]The warm sea-ice or snow albedo is the albedo at a temperature of 0°C.
[d]Albedos are linearly interpolated for temperatures between the cold albedo temperature and 0°C.
[e]For ice thinner than the albedo thickness scale, the sea-ice albedo is a mixture of the ocean albedo and the sea-ice albedo calculated from temperature alone. The snow thickness scale is the water equivalent depth of snow above which the surface albedo is at least a 90% mixture of the snow albedo. The albedos listed here represent the broadband averages. This means that when the model has both visible and infrared albedos, we calculate the broadband average albedo assuming 40% of the sunlight reaching the surface is visible and the rest is infrared.
[f]SNOWMIP is not a model, but rather a set of standard albedos applied to all models participating in the intercomparison. In the case of ECHAM5, the snow albedo is not used, because ECHAM5 does not incorporate snow cover on sea ice. SNOWMIP "constant albedo" runs set the snow albedo to the SNOWMIP sea-ice albedo.

simulation of circulation and clouds. This claim is reinforced by the fact that when the snow and ice albedos are both set to 0.6, ECHAM5 produces a higher global ice fraction at all CO_2 levels and has a higher threshold CO_2 for initiation than does either FOAM or CAM (**Figure 4*c***).

The threshold CO_2 for initiation is drastically lower for ECHAM5/MPI-OM than it is for ECHAM5, which implies that initiating a Snowball in the fully coupled model is much harder. If anything, one might have expected ECHAM5/MPI-OM to initiate more easily than ECHAM5, because ECHAM5/MPI-OM incorporates the effects of high-albedo snow over sea ice (**Table 3**). The relative difficulty of Snowball initiation in the fully coupled model is likely due to the effects of the dynamic ocean, which can transport heat horizontally to the ice margin to prevent the equatorward spread of ice (Poulsen & Jacob 2004, Poulsen et al. 2001).

Both ocean heat transport and a low ocean-ice albedo contrast help allow states that have nonzero ice coverage but that fall short of becoming a full Snowball. For example, ECHAM5/MPI-OM produces states with intermediate ice coverage that exist for wide ranges of CO_2 and are easy to find (**Figure 4*a***), whereas the SNOWMIP models mostly do not, when run with default and SNOWMIP albedos (**Figure 4*a,b***). This likely results from the stabilizing effect that sharp gradients in ocean heat transport have on a sea-ice margin (Rose & Marshall 2009). The effect of ocean-ice albedo contrast on the existence of intermediate states in GCMs is captured well by one-dimensional EBMs of the sort discussed in Section 3.3. Snowball initiation is far easier in fully coupled ECHAM5/MPI-OM than it is in fully coupled FOAM. For example, a Snowball initiates in FOAM for a solar constant between 91% and 92% of modern values when $CO_2 = 140$ ppmv and $CH_4 = 700$ ppb and when the model is run with idealized Neoproterozoic boundary conditions (Poulsen & Jacob 2004). This contrasts with ECHAM5/MPI-OM, in which a Snowball initiates for a solar constant between 95.5% and 96% of modern values when $CO_2 = 278$ ppmv,

$CH_4 = 650$ ppb, and $N_2O = 270$ ppb, and when the model is run with realistic Neoproterozoic boundary conditions (Voigt et al. 2010). SNOWMIP allows us to understand, to a certain extent, the reasons for this. First, because it is easier to initiate a Snowball in ECHAM5 than in FOAM with SNOWMIP boundary conditions and default albedos (**Figure 4*a***), the difference between initiation in ECHAM5/MPI-OM and initiation in fully coupled FOAM cannot be due solely to differences in the simulation of ocean dynamics. Second, the SNOWMIP constant-albedo simulations (**Figure 4*c***) establish that differences in the simulation of cloud and atmospheric dynamics must also be a significant part of the initiation discrepancy between ECHAM5/MPI-OM and fully coupled FOAM.

The robust result common to both coupled models is that, all other things being equal, ocean dynamic heat flux greatly lowers the CO_2 threshold required for initiation. This happens because ocean mixing approximately homogenizes the tropical temperatures, making it impossible for the oceans to freeze over until the entire tropics are reduced to freezing. The Hadley cell is effective at bringing about this kind of homogenization in the atmosphere, but the coupling of surface temperature to air temperature is not tight enough to inhibit freezing with atmospheric transport alone.

The SNOWMIP simulations establish that snow plays a key role in Snowball initiation. In both SNOWMIP models that simulate snow on sea ice, CAM and FOAM, the threshold CO_2 for initiation is far lower when both snow and sea-ice albedos are set to 0.6 than when the sea-ice albedo is set to 0.6 and the snow albedo is set to 0.9 (cf. **Figure 4*b*,*c***). Furthermore, without snow, the ocean-ice albedo contrast is low enough that states with intermediate ice coverage exist and are stable even without ocean heat transport (**Figure 4*c***).

The SNOWMIP results establish that it would be easy to enter a Snowball without ocean dynamics and that snowfall increasing the albedo of sea ice is essential for Snowball initiation. They also show that atmospheric dynamics and cloud simulation are at least part of the reason that ECHAM5/MPI-OM enters a Snowball more easily than does fully coupled FOAM. The SNOWMIP results do not allow us to say whether the ECHAM5/MPI-OM or fully coupled FOAM results are more realistic for Snowball simulation, although it is fair to note that ECHAM5/MPI-OM is one of the most sophisticated global climate models and has a much more detailed cloud parameterization than does FOAM (although no cloud parameterization to date has been specifically designed with Snowball conditions in mind). The fact that one of the world's most sophisticated climate models enters a Snowball relatively easily demonstrates that there are no robust physical barriers to initiation.

4.2. Mechanisms for Initiation

There are no completely satisfactory mechanisms that account for the initiation of Snowball events. In particular, none of the proposed mechanisms explains why glaciations resume in the Neoproterozoic after a billion-year absence. All the proposed mechanisms invoke some mechanism for drawing down CO_2 through geochemical or biogeochemical processes. The essential problem is accounting for the breakdown of Earth's silicate weathering thermostat, which normally keeps the planet from freezing over. An important point concerning the thermostat: There are indications that, without the soil organic acids produced by land plants, the weathering rate becomes directly dependent on p_{CO_2} instead of just indirectly dependent on p_{CO_2} via its effect on temperature and rainfall (Brady & Caroll 1994). The direct dependency makes the silicate weathering thermostat less effective and therefore makes the system more prone to breakdown, especially on the cold side (Pierrehumbert 2010, chapter 8). If this is indeed a factor, it would imply that Earth continued to be vulnerable to Snowball glaciations up through the time land plants became common in the

Silurian (444–416 Mya)—and that the absence of Phanerozoic low-latitude glaciation events was either a matter of luck or the intervention of some other process.

The absence of carbonate-precipitating plankton in the open ocean is another factor that could have made the younger Earth more susceptible to Snowball glaciation; in the absence of such organisms, there would be less buffering of ocean pH by sedimentary carbonate dissolution, and this would make it easier to draw down atmospheric CO_2 (Ridgwell et al. 2003). However, because biomineralizing nannoplankton have been around only for the past 250 million years or less, this does not explain what was special about the Neoproterozoic.

It has been proposed that the extreme Neoproterozoic glaciations occur because the concentration of continental area in the tropics allows them to continue drawing down CO_2 by silicate weathering until the ice margin invades the tropics (Hoffman & Schrag 2002), by which time global glaciation may become inevitable. This is a plausible mechanism in light of the tropical continental precipitation patterns seen in models. Tropical supercontinents get little precipitation in their interiors, but silicate weathering is enhanced greatly when they break up. In the Phanerozoic, this process leads to cooling during the breakup of Pangea but not to the extreme glaciations seen in the Neoproterozoic (Donnadieu et al. 2006). Perhaps the difference is due to the effect of land plants on the silicate weathering thermostat and also is connected with the brighter Sun.

The tropical weathering hypothesis begs the question of why Snowball or Waterbelt glaciations were avoided at other periods with a lot of tropical continental area (e.g., approximately 580 Mya). Knowledge of continental distribution during the Boring Billion period is sketchy, but it would provide a crucial test of the tropical weathering hypothesis.

The fire-and-ice mechanism (Godderis et al. 2003) is a variation on the theme of tropical silicate weathering. In this mechanism, invoked as a cause of the Sturtian glaciation, the massive tropical flood basalts that accompanied the breakup of Rodinia provided an anomalously great supply in the tropics of fresh, highly weatherable rock surface, which accelerated silicate weathering. This begs the question of what caused the later Marinoan glaciation because there were no new emplacements of flood basalts at the time. It seems unlikely that leftover basalt from the Sturtian played a role in the initiation of the Marinoan because the postglacial hothouse following the Sturtian would provide an ideal environment for consuming the remaining highly weatherable surface, whence the leftover basalts would, at best, accelerate the recovery of the postglacial hothouse to a more normal climate. The fire-and-ice mechanism has been tested within a highly parameterized EBM (Godderis et al. 2003), but given the importance of precipitation to weathering rates and the unreliability of precipitation parameterizations in EBMs, the viability of the mechanism needs to be tested with GCMs along the lines of the asynchronously coupled weathering study in Donnadieu et al. (2006). The same remark applies to the tropical weathering hypothesis in general, regardless of the role of flood basalts.

Net sequestration of organic carbon produced by oxygenic photosynthesis provides another way to draw down CO_2. It works through the conversion of CO_2 to O_2, and the net burial of the resulting organic carbon would be manifest in the record as a positive $\delta^{13}C$ excursion in carbonates. To get initiation via organic carbon sequestration, the burial must happen on a timescale fast enough that the reduction in CO_2 is not offset by resupply from volcanic outgassing. This would typically require drawdown on a timescale less than a few hundred thousand years. The idea that photosynthetic carbon burial could draw down CO_2 rapidly is far from fanciful. After all, in the modern world, photosynthesis fixes carbon at a rate that could deplete the atmospheric CO_2 inventory in a matter of decades, and the atmosphere-ocean inventory in a matter of a few thousand years. This does not happen because respiration recycles organic carbon into CO_2 about as quickly as photosynthesis fixes organic carbon. The key question regarding oxygenation and CO_2 drawdown, then, is whether a sufficiently large fraction of the carbon fixed by photosynthesis

each year can be sequestered in a place where it is protected from oxidation (and also sulfate reduction).

In addition to CO_2, the other major long-lived greenhouse gas in play is CH_4. The joint photochemistry of the two is also the key player in organic haze formation (Trainer et al. 2006). Organic haze intercepts sunlight before it reaches the ground, and it can therefore reduce surface temperature. Some methane can outgas from Earth's interior, but in the Neoproterozoic, the most significant source would probably have been methanogenic bacteria. Once there is significant O_2 in the atmosphere, as was the case in the Neoproterozoic, CH_4 can rapidly oxidize to CO_2 and water vapor. The reaction is not a simple combustion reaction because, at typical atmospheric temperatures, it must be catalyzed by the OH radical to proceed at a significant rate. Determination of methane lifetime, therefore, is not a simple thing because it engages the full atmospheric chemistry that determines the concentration of OH (Yung & DeMore 1999). This chemistry causes methane lifetime, and hence methane concentration, to increase nonlinearly with the rate of methane production as the OH radical becomes progressively depleted (Pavlov et al. 2003).

Organic haze: a smog of particles composed of complex organic molecules, which reflect and absorb solar radiation

The methane-shotgun mechanism (Schrag et al. 2002) attempts to explain the preglacial negative $\delta^{13}C$ excursion through a sustained release of methane stocked in clathrates (leading to a greenhouse effect supported mostly by methane rather than CO_2) followed by a collapse of methane through oxidation to CO_2 once the source is exhausted. In the first stage of this scenario, CO_2 is driven to low values because the high methane concentration keeps the climate warm enough to support a high rate of silicate weathering, even when CO_2 is low. The silicate weathering thermostat adjusts CO_2 to compensate for the enhanced methane flux much as it works to compensate for the Faint Young Sun.

The methane-shotgun mechanism for initiation rests in part on a widely held misconception of the potency of methane as a greenhouse gas. In Earth's present atmosphere, it is valid to think of methane as, molecule for molecule, a stronger greenhouse gas than CO_2, but it is often forgotten that this property is concentration dependent. For example, Schrag et al. (2002) assume a fixed 21:1 radiative equivalent between methane and CO_2. In reality, the high CO_2 equivalent of methane in the present climate is mainly because the methane concentration is small compared with CO_2 and because the radiative effect of both gases is nearly logarithmic in concentration. Methane looks like a stronger greenhouse gas simply because fewer molecules are required to double its concentration than are necessary to double CO_2, which starts from a higher initial value. Actually, methane is intrinsically a worse greenhouse gas than CO_2 because it absorbs in a spectral region that is fairly far from the peak of Earth's thermal emission. The misconception was compounded by an error in the radiation code of Pavlov et al. (2000) that exaggerated the effect of methane at high concentrations (see discussion and correction in Haqq-Misra et al. 2008). As an independent check, we have recomputed the methane radiative transfer directly from the high-resolution transmission molecular absorption (HITRAN) spectroscopic database (as described in Pierrehumbert 2010, chapter 4). For a test case consisting of a dry air adiabat that has a surface temperature of 280 K and that is mixed only with methane or CO_2, the *OLR* is 331 W m^{-2} for 100 ppmv of methane versus 313 W m^{-2} for 100 ppmv of CO_2. These compare with 349 W m^{-2} for an infrared-transparent atmosphere, which has no greenhouse effect. The CO_2 has a much stronger greenhouse effect than does the methane, and oxidation of a methane-dominated greenhouse atmosphere into a CO_2-dominated greenhouse atmosphere would actually warm the planet if all the resulting CO_2 were to remain in the atmosphere. We have run the same test case using the NCAR CCM3 radiation code (Kiehl & Briegleb 1992, Kiehl et al. 1998) and found nearly identical numbers. Hence in the following, we feel justified in using the CCM3 code to deal with cases involving multiple greenhouse gases and water vapor, up to 100 ppmv of methane.

As an example of how the methane-shotgun idea might work given the revision in the radiative transfer, let us suppose that the atmosphere starts with 2,000 ppmv of CO_2 and no methane. The ECHAM5/MPI-OM model, including dynamic ocean heat transports, stays out of a Snowball under these conditions (see **Figure 4*a***). Using the CCM radiation code with 50% relative humidity, and assuming the temperature profile to be on the moist adiabat with an isothermal stratosphere as in the *OLR* calculation of Section 3, the *OLR* for a surface temperature of 285 K is 252 W m^{-2}. If we then add 100 ppmv of methane, the *OLR* would drop to 240 W m^{-2}, unbalancing the energy budget. Earth would warm up to balance the budget, but then the increased temperature and precipitation would increase silicate weathering until the CO_2 was drawn down and equilibrium was restored at something approaching the original temperature. If the silicate weathering thermostat perfectly compensated for the added methane, the temperature would remain unchanged, with the CO_2 driven down to 350 ppmv. However, given the direct p_{CO_2} dependency of weathering in the absence of land plants, the weathering rate goes down with p_{CO_2} even if temperature and precipitation remain fixed, so the equilibrium would be hotter and the CO_2 concentration would not go down as much as it does in the perfect compensation case. Still, let us assume that the CO_2 goes all the way down to 350 ppmv but that the methane source then ceases abruptly, so that the 100 ppmv of methane oxidizes to CO_2. As noted by Schrag et al. (2002), almost all the excess CO_2 produced this way would be taken up by the ocean on a timescale of 10,000 years or so; hence we ignore the greenhouse effect from the additional CO_2. We are then left with the greenhouse effect of 350 ppmv of CO_2, plus the water vapor corresponding to the assumed temperature. In ECHAM5/MPI-OM, this is just barely adequate to initiate a Snowball (**Figure 4*a***). It thus appears that the methane-shotgun mechanism, from a radiative standpoint, is still in play, but it has a fairly narrow window of conditions in which it can operate. Several factors could make the mechanism fail, including failure to draw down CO_2 to the full compensation value, some residual methane, or a somewhat lower ice/snow albedo. There are two serious problems with the methane-shotgun mechanism: (*a*) It is far from clear that enough methane could be stocked in clathrates to sustain elevated methane concentrations for the several hundred thousand years needed for silicate weathering to draw down the CO_2, and (*b*) it is not clear that enough methane could be released gradually enough to do the trick.

Alternately, the initially elevated methane concentration could arise from a steady-state response to greatly enhanced net biological methane production. Pavlov et al. (2003) suggest that this might have happened as a result of reduced methanotrophy, leading to Proterozoic methane concentrations in the range of 100 to 300 ppmv. It is unlikely, however, that this scenario could produce the negative ^{13}C excursion that precedes the glaciations. A collapse of even 300 ppmv of atmospheric methane by oxidation to CO_2 in the atmosphere or bicarbonate in the ocean would not produce much of a negative isotopic excursion because the stock of light carbon in the atmosphere is too small (approximately 600 Gt) in comparison with the oceanic inorganic carbon reservoir. But what is the isotopic situation in a steady state, in which methanogenesis is balanced by methane oxidation and the atmospheric methane concentration is constant? When methanogenesis produces isotopically light methane using CO_2 or organic carbon as a feedstock, it leaves behind isotopically heavy bicarbonate or CO_2. This reservoir mixes back with the isotopically light CO_2 or bicarbonate produced by methane oxidation, canceling out the isotopic signature of methanogenesis. At the extreme limit in which methanogenesis intercepts all organic carbon produced by photosynthesis and then converts it to methane, which then oxidizes to CO_2 or bicarbonate, the situation is just as if no organic carbon were being buried at all; the $\delta^{13}C$ of sedimentary carbonates would revert to –6‰ in this case. The situation would be isotopically indistinguishable from one in which all the organic carbon is directly oxidized by respiration or sulfate reduction.

5. CLIMATE OF THE SNOWBALL STATE

The overarching feature of the Snowball climate is that the replacement of the ocean with a globally thick ice cover eliminates the ocean's thermal inertia. The low thermal inertia of the Snowball surface results in an extreme seasonal cycle in which the surface temperature pattern responds largely to the instantaneous distribution of absorbed solar radiation rather than to the annual mean. As noted by Walker (2001), the seasonal cycle is rather like that of Mars, which also has a global solid surface. The Martian analog is strengthened by the fact that the solar radiation absorbed by the high-albedo Snowball Earth, per unit surface area, is comparable to the solar radiation that the non-Snowball Mars absorbs in its more distant orbit. The Neoproterozoic solar forcing of the Snowball is 128 W m^{-2} if the albedo is 60%, or 96 W m^{-2} if the albedo is 70%; this compares with 110 W m^{-2} for present Mars or approximately 77 W m^{-2} for the Mars of 4 billion years ago. Furthermore, at the low temperatures of Snowball Earth and Mars, the water vapor content of the atmosphere is so low that neither the water vapor greenhouse effect nor the latent heat of water vapor condensation has any significant influence on the climate. The Snowball climate differs from present Mars, however, in that Earth's atmosphere is thicker, providing enough thermal inertia to damp the diurnal cycle significantly; in this regard, Snowball Earth is more like an early Mars with a dense atmosphere. A further difference is that Earth is a larger planet. Given the same rotation rate, this means that Earth's Hadley cell is more confined to the tropics, whereas that of Mars has a more global character—all other things being equal, a larger planet acts dynamically like a more rapidly rotating planet of lesser diameter (Caballero et al. 2008).

Pierrehumbert (2005) gives a comprehensive account of the climate of the Snowball state on the basis of analysis of a series of GCM simulations. Here we illustrate some of the key properties of the Snowball climate using globally glaciated states obtained from the simulations described in Section 4.1. **Figure 5** shows the January surface air temperature for a series of simulations that were

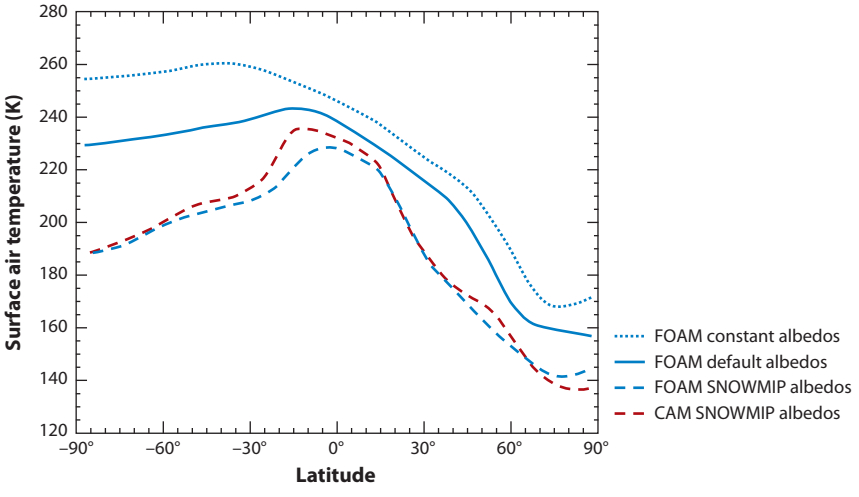

Figure 5

January surface air temperature for several general circulation model (GCM) simulations of the Snowball state, with CO_2 at 2,000 ppmv. The FOAM default albedo case uses the model's default albedo parameterization, given in **Table 3**. The SNOWMIP cases use an albedo of 0.6 for sea ice and 0.9 for snow. The constant-albedo case uses an albedo of 0.6 for both ice and snow. Abbreviations: CAM, National Center for Atmospheric Research's Community Atmosphere Model v3.1; FOAM, Fast Ocean Atmosphere Model v1.5; SNOWMIP, Snowball model intercomparison.

carried out with a CO_2 concentration of 2,000 ppmv and that employed two different GCMs and a variety of assumptions about the albedo of ice and snow. Results for the Southern Hemisphere winter solstice (July) look the same, except they are reflected about the equator. Looking first at the FOAM constant-albedo simulation, we see the expected extreme seasonal cycle, as indicated by the large temperature difference between the winter (Northern) and summer (Southern) hemispheres. The summer hemisphere temperature is uniform, simply because the insolation pattern is fairly uniform in summer for Earth-like obliquities. In the SNOWMIP simulations, the high-albedo snow cover brings down the summer extratropical temperatures considerably; CAM and FOAM give similar results when run with identical albedo parameters, despite the fact that the resolution and cloud schemes differ. CAM runs approximately 10°C warmer than does FOAM in the summer hemisphere, primarily due to a greater cloud greenhouse effect, but even CAM is well below freezing at 2,000 ppmv. The differences between CAM and FOAM are swamped by the effect of changing the snow albedo, however. This can be seen in the run with the FOAM default albedo, which uses a smaller (and more realistic) snow albedo than that used by the SNOWMIP runs.

The EBMs discussed in Section 3 made it clear that the temperature of the Snowball state is affected greatly by the surface albedo. The GCM results underscore the importance of snow cover in controlling the albedo. Differences in albedo assumptions among models almost certainly account for a great deal of the differences among simulated Snowball states. For example, the snow-aging parameterization in the Laboratoire de Météorologie Dynamique GCM (LMDz) reduces the albedo of old snow and makes the climate more like the constant-albedo (0.6) FOAM simulation shown in **Figure 5** (Le Hir et al. 2010). It is unclear whether the snow-aging model used in LMDz is valid for the low temperatures and sluggish hydrological cycle of the Snowball, but the results drive home the extreme importance of developing better models of the Snowball surface.

The low thermal inertia of the surface also gives the Snowball state a Mars-like extreme diurnal cycle. The thick Snowball atmosphere has sufficient thermal inertia to keep the free troposphere from having much of a diurnal cycle, but the surface nonetheless cools dramatically at night because there is little turbulent heat flux through the stable boundary layer and because the downward infrared flux from the cold, dry atmosphere is fairly weak. For example, for an atmosphere with a surface temperature of 230 K, a CO_2 concentration of 2,000 ppmv, and a relative humidity of 70%, a simple calculation with the CCM radiation model shows that the downward infrared flux to the surface is only 57 W m^{-2}. In blackbody equilibrium, this maintains a surface temperature of only 178 K.

The main factor that keeps the surface from dropping to its nighttime equilibrium value is the diffusion of heat to the surface from the warmer subsurface layers. Most GCM ice models do not have sufficient resolution to represent this process properly and therefore exaggerate the diurnal cycle (Abbot et al. 2010). Coarse vertical resolution limits the maximum thermal gradient that can be attained and therefore reduces the diffusive flux that warms the surface. In the daytime, a similar process works to produce excessive daytime warming. This can lead to spurious deglaciation through the diurnal melt-ratchet process (discussed in Section 6). The problem is even more pronounced when the snow cover is thick because of the low thermal diffusivity in snow. On the basis of Fourier's solution, the thermal anomaly penetrates to a characteristic depth of $\sqrt{D/\omega}$ in a solid, where D is the diffusivity and ω is the angular frequency of the surface temperature perturbation. With $D = 0.38 \cdot 10^{-6}$ m^2 s^{-1} (appropriate to dry snow), the diurnal cycle penetrates only ~7 cm into the snow. Given that it is common for GCM snow models to have only a single layer, inaccuracies often result when the snow thickness exceeds a physical depth of 10 cm, which corresponds to a liquid water equivalent of 3 cm or less. The excessively low nighttime temperatures lead to spurious estimates of the threshold for CO_2 condensation at the surface. Broadly speaking,

there are indications that the overestimated diurnal cycle does not seriously affect the conditions for deglaciation until diurnal melt begins to occur, but the situation requires further study.

A few other distinguishing features of the Snowball climate need to be noted. Because of the high surface albedo, the proportion of solar energy that is absorbed directly within the atmosphere without having to be first absorbed at the surface and then communicated upward by convection is large compared with climates featuring a preponderance of open water. Strong absorption of solar radiation high in the atmosphere can have an antigreenhouse effect, as seen on Titan, and can cool the surface (McKay et al. 1999). Absorption in the lower troposphere, however, acts equivalently to a reduction in surface albedo. Le Hir et al. (2010) highlighted the effects of solar near-infrared absorption by CO_2, which may not be properly represented in GCM radiation codes when the CO_2 concentration approaches the high values needed for deglaciation. We have found this effect to be modest in comparison with near-infrared absorption by water vapor (Pierrehumbert 2010, chapter 5), although one always must be wary of the possibility that GCMs might exaggerate solar absorption by CO_2 when they are used outside their intended range. The solar absorption by water vapor becomes particularly important in a Snowball climate because the very low water vapor content allows solar near infrared to penetrate deep in the atmosphere and be absorbed near the surface. This contrasts with the modern climate, in which solar near infrared in bands that can be absorbed by water vapor is mostly exhausted by the time it reaches the upper troposphere.

The vertical temperature structure of the atmosphere is also of interest, not least because a weak vertical gradient suppresses the greenhouse effect. As noted in Pierrehumbert (2004, 2005), the atmosphere in the winter hemisphere is close to isothermal, except near the surface, where there is a temperature inversion. Latitude-height plots showing the vertical structure of selected Snowball state simulations are shown in **Figure 6**. The FOAM constant-albedo case, which has a relatively strongly absorbing ice surface, shows the interhemispheric dichotomy well; it features an isothermal profile in the winter hemisphere extending to 30 N and a polar winter inversion, but a convection-driven troposphere in the summer hemisphere exhibiting a temperature decrease with height. Even in the summer hemisphere, though, the vertical temperature contrast is weak compared with the warm, moist Earth of today, amounting to 70 K at most, in comparison with

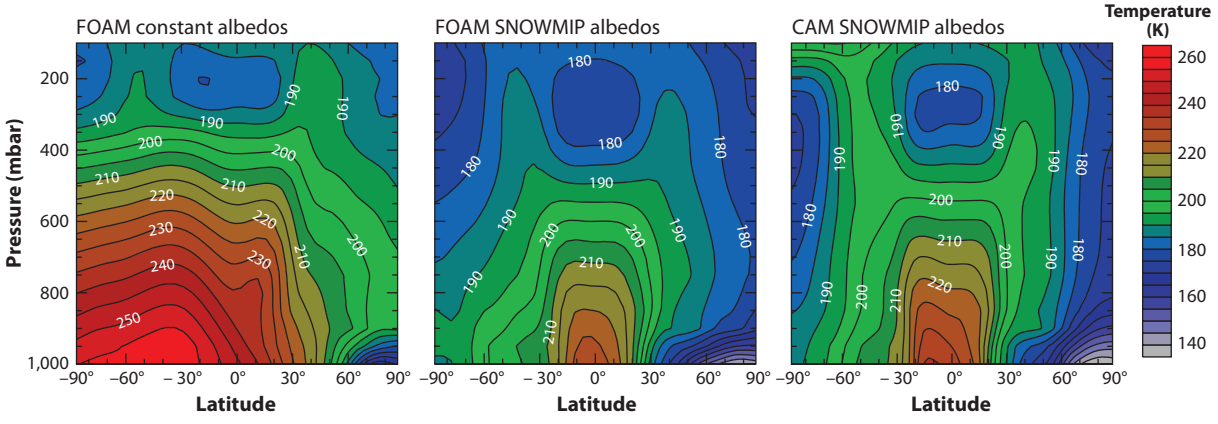

Figure 6

Latitude-height patterns of January zonal mean temperature for $CO_2 = 2{,}000$ ppmv. (*Left*) FOAM constant-albedo simulation. (*Middle*) FOAM SNOWMIP-albedo simulation. (*Right*) CAM SNOWMIP-albedo simulation. Vertical coordinate is pressure in millibars (mbar). Abbreviations: CAM, National Center for Atmospheric Research's Community Atmosphere Model v3.1; FOAM, Fast Ocean Atmosphere Model v1.5; SNOWMIP, Snowball model intercomparison.

Meteoric ice: ice formed from compacted snow

110 K in the modern tropics. In the SNOWMIP runs, the high-albedo snow surface suppresses convection and the consequent adiabatic lapse rate even in the summer extratropics, and strong vertical temperature contrasts exist only in the tropics. CAM and FOAM simulations of this situation look similar, despite the differences in horizontal resolution, vertical resolution, and cloud schemes. In the SNOWMIP runs, the high albedo and low thermal inertia of the snow allow the inversion layer to extend all the way to the edge of the winter subtropics. The temperature structure in the winter hemisphere in all cases implies that the atmosphere there has an unusually high static stability compared with the present-day troposphere. This has dynamical consequences, because the Rossby radius of deformation is proportional to the static stability, and both synoptic eddies and Rossby waves have characteristics that scale with that length. In some sense, the whole winter hemisphere acts as if it were all stratosphere—a feature that is also rather Mars-like.

The low summer tropopause and weak vertical temperature contrast are a fairly straightforward consequence of the fact that the near absence of water vapor makes the atmosphere optically thin (Pierrehumbert 2010, chapter 4). Venus provides the opposite extreme of this effect, with an optically thick atmosphere and a vertical temperature contrast of more than 500 K.

The winter stratification is a more delicate matter. Atmospheric solar absorption and the warming effect of atmospheric lateral dynamic heat fluxes were highlighted as contributing factors in Pierrehumbert (2005), but we have since found, through experimentation with radiative-convective models, that the seasonal cycle also plays a major role. This happens because the high, cold atmosphere has a longer radiative relaxation time than the lower atmosphere, so that in the course of the seasonal cycle, the low-level air cools faster than the upper-level air. This effect is seen clearly in **Figure 6**, where the temperature hovers around 190 K globally at 200 mbar, whereas the lower atmosphere exhibits strong winter/summer gradients. There appears to be some model dependency in the degree of winter stratification (see, e.g., Le Hir et al. 2007), but some of this may be driven by differences in albedo rather than differences in the radiation schemes or dynamics. Certainly, convection parameterizations should play only a small role because there is essentially no convection in the winter hemisphere.

5.1. The Snowball Hydrological Cycle

Snowball states have a sluggish but vital hydrological cycle, fed by sublimation from the snow or ice surface. The hydrological cycle transforms sea ice into water vapor, which is transported through the atmosphere and redistributed over the surface as meteoric ice. At the low temperatures of Snowball states, the evaporation is limited by the low-saturation water vapor pressure yielded by the Clausius-Clapeyron relation (Pierrehumbert 2002). The latent heat flux carries little energy away from the surface, and the rate at which water fluxes through the system is small. Yet the slow redistribution of water has a profound effect on ice ablation and on the surface albedo, which is determined largely by snow cover.

The annual mean precipitation minus evaporation ($P - E$) pattern for a typical Snowball state is shown in **Figure 7**. The basic structure of the Snowball hydrological cycle consists of a net ablation zone near the equator and a transport of water toward the poles. This is exactly the opposite of the pattern familiar from the modern climate, or indeed any climate with an unglaciated tropics. The difference arises from the low thermal inertia of the Snowball surface, which causes the upward branch of the Hadley circulation (the intertropical convergence zone, or ITCZ) to undergo an extreme seasonal excursion from the northern to the southern subtropics. Because the ITCZ spends more time at the extremes, moisture is carried systematically to the edge of the tropics, where it can be further redistributed by synoptic eddy transports. The process is identical to the process that accounts for the poleward transport of methane on Titan (Mitchell 2008), except that

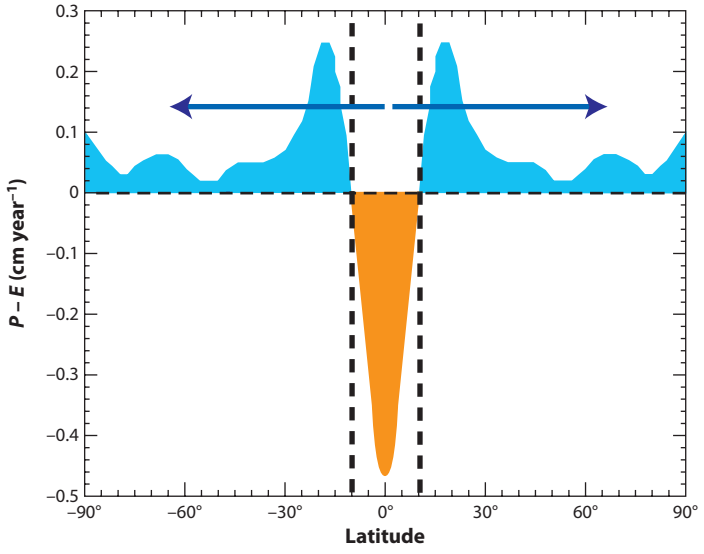

Figure 7

Annually averaged zonal mean precipitation minus evaporation ($P - E$) for the Fast Ocean Atmosphere Model v1.5 (FOAM) default-albedo Snowball state at 2,000 ppmv CO_2. Results are averaged over only a single year, but there is little interannual variability.

in that case the low rotation allows the ITCZ excursion to extend all the way to the poles. The presence of a net ablation zone centered on the equator is robust, but the precise width of the ablation zone is model dependent (Abbot & Pierrehumbert 2010).

The small $P - E$ in **Figure 7** is actually the residual of precipitation and evaporation values that are individually an order of magnitude larger. Most of this represents water that sublimates and then precipitates out locally in the course of the diurnal cycle. Because $P - E$ scales with the moisture transport, it increases exponentially in accord with the Clausius-Clapeyron relation as temperatures warm toward deglaciation, as long as the relative humidity remains roughly constant and the strength of the circulation does not change much. With this scaling, warming the tropical surface from 250 K to 270 K would increase $P - E$ by a factor of 6.4.

As sluggish as it is, the Snowball hydrological cycle is crucial to explaining the presence of glacial deposits (diamictites) in Snowball stratigraphic sequences. These require active land glaciers discharging into the ocean, and the only way to build such glaciers is by snowfall. Even modest snowfall is sufficient to cover the continents with glaciers whose ice streams have sufficient erosive power to explain the diamictites (Donnadieu et al. 2003). The calculation has never been done with a fully coupled glacier/climate model, though, and requires further study.

5.2. Ice Thickness

How thick is the sea ice in a Snowball state? The simplest calculation balances the geothermal heat flux delivered to the base of the ice against heat diffusion through the ice. The ice thickness takes on a value that is just enough to let the required amount of heat through, as sketched in **Figure 8**. The basal temperature is assumed to be the freezing point of seawater, and the surface temperature is determined by the planetary and surface energy balance. For uniform thermal conductivity, the ice thickness is $\kappa \Delta T / F_b$, where F_b is the basal flux, κ is the thermal conductivity, and ΔT is the

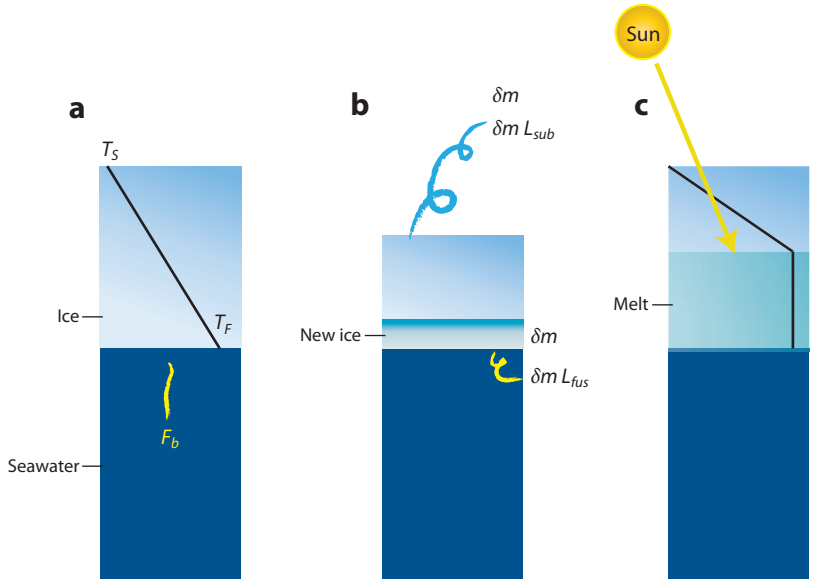

Figure 8

Basic physics determining ice thickness. (*a*) Ice thickness determination by balance between heat flux applied at base and heat diffusion through ice. (*b*) Effect of sublimation at surface balanced by freezing at base, which applies additional basal flux from release of latent heat of fusion. (*c*) Ice thinning due to deposition of solar energy in the interior of the ice, which increases the thermal gradient and leads to melting of the deep ice. Symbols: F_b, basal flux; L_{fus}, latent heat of fusion; L_{sub}, latent heat of sublimation; T_F, freezing temperature of sea water; T_S, surface temperature; δm, mass of new ice added.

temperature difference across the ice layer. Using $\kappa = 2.2$ W m^{-1} K^{-1} and $F_b = 0.05$ W m^{-2}, the thickness is 880 m for tropical conditions with $\Delta T = 20$ K and 3,080 m for polar conditions with $\Delta T = 70$ K. This is more like a land ice sheet or the thick ice crust of Europa than it is like the thin sea ice familiar from the Phanerozoic climate.

Despite the cold temperatures in a Snowball, there is significant net sublimation from the tropical ice, and in a steady state, this mass loss must be balanced by formation of new ice at the base of the ice layer. As indicated in **Figure 8**, this process leads to an upward flow in the ice and transport of water from the sea to the surface, where it enters the atmosphere by sublimation. This process is known as the sea-ice elevator. The freezing of ice at the base releases latent heat at a rate equal to the sublimation mass loss per square meter of surface times the latent heat of fusion. For a typical sublimation rate of 2 cm year^{-1}, this yields a basal heat flux of 0.21 W m^{-2}, which is sufficient to thin the tropical ice to 170 m when added to the geothermal heat flux.

The penetration of solar radiation deep into the ice, where it is absorbed, has the potential to reduce the ice thickness dramatically. Solar penetration works through a form of "solid greenhouse" effect, in that shortwave radiation penetrates easily into the interior of clear ice, but the resulting heat can get to the surface and escape only slowly, through molecular diffusion (which plays the role that infrared opacity plays in the atmospheric greenhouse effect). An elementary treatment of the process is given in chapter 6 of Pierrehumbert (2010). The deposition of energy in the interior of the ice can raise the subsurface ice temperature to the melting point, preventing the ice from growing beyond the thickness where such melting occurs. McKay (2000) proposed that solar penetration could lead to Snowball solutions with thin, clear tropical ice only a few

meters thick and suggested that the resulting penetration of light into the tropical ocean would be the means by which photosynthetic life (especially eukaryotes) could survive the Snowball state. However, the degree of solar penetration needed to maintain thin ice requires clear, bubble-free ice, lest the sunlight scatter back before it can penetrate very far. Moreover, spectrally resolved calculations of radiative transfer in ice do not support the form of absorption profile needed for thin ice (Warren et al. 2002). Some GCMs incorporate the solar penetration effect, but one must be wary of results that depend on this process because the representation, if present at all, typically has poor spectral resolution and may exaggerate the effect.

5.3. Sea Glaciers

The thick sea ice of the Snowball state deforms under the compressional stress of its own weight, leading to a flow that is more like a global version of the Ross Ice Shelf than it is like the flow of modern, thin sea ice. For floating ice, the basal stress is very small, so there is essentially no vertical shear in the ice flow. The flow is like that occurring in a ball of dough being compressed when the baker pushes down on it from above (see **Figure 9**), except that one has to imagine that the top and bottom are well greased and free to slide. Unlike frozen-bed land ice sheets, sea-glacier flow is not driven by

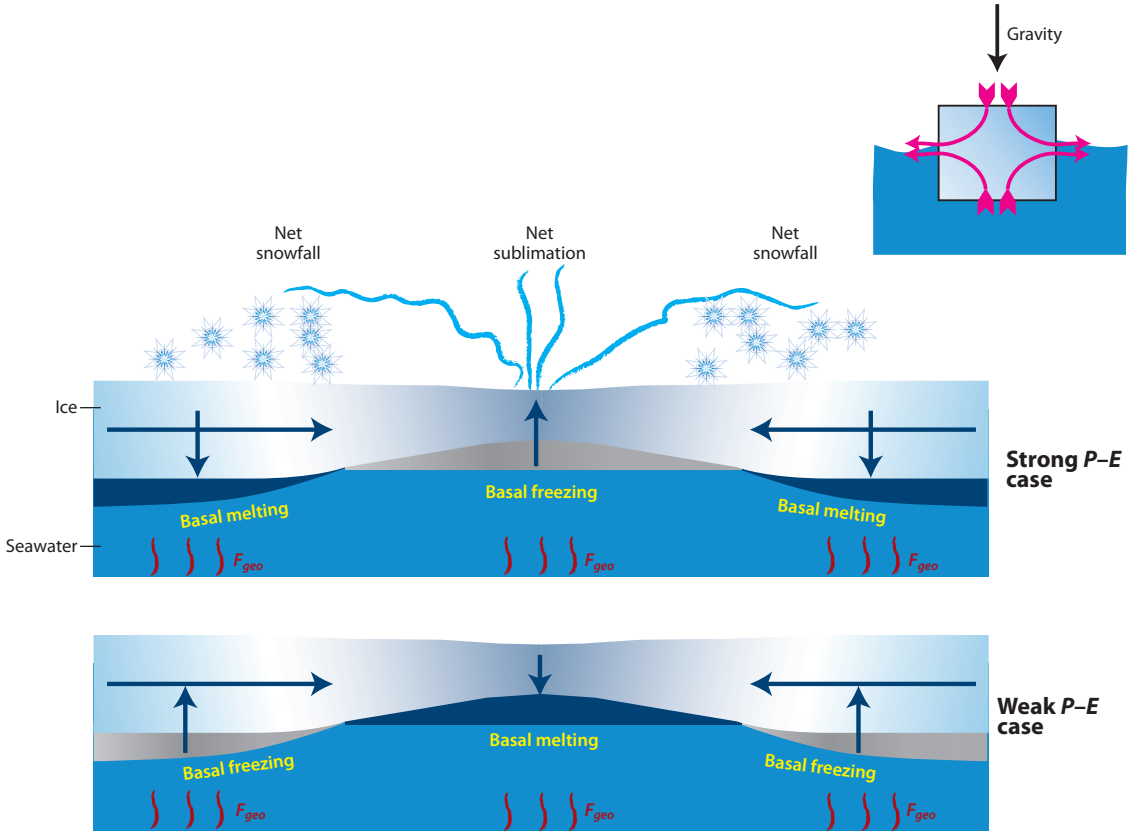

Figure 9

Schematic of sea-glacier flow in the weak precipitation minus evaporation ($P - E$) limit (*lower panel*) and strong $P - E$ limit (*upper panel*). The inset illustrates the way deformation under gravity causes the ice to flow. Symbol: F_{geo}, geothermal heat flux.

local pressure gradients arising from horizontal variation of the ice thickness. The behavior of sea glaciers in Snowball and Waterbelt states was first examined in Goodman & Pierrehumbert (2003).

Sea glaciers are composed of two distinct kinds of ice: sea ice that most recently originated from the freezing of seawater, and meteoric ice that has been processed by sublimation, precipitation, and consolidation into firn and eventually glacier ice (Goodman 2006). Sea glaciers transport water and can be regarded as one of the branches of the hydrological cycle. Let us first consider the case in which the atmospheric moisture transport is negligible, so that $P - E$ can be regarded as zero (**Figure 9**). Without ice flow, the ice thickness would grow until the local equilibrium thickness is reached. Because the surface is colder toward the poles, the equilibrium thickness is greatest at the poles and thinnest toward the equator. The equatorward flow in the sea glacier, however, causes the ice to be thinner than its equilibrium value in polar regions, so that new ice forms there by freezing onto the base. Similarly, the ice is thicker in the tropics than its local equilibrium, so excess ice melts at the base. The sea glacier carries water equatorward, with a poleward return branch in the ocean. If there were truly no atmospheric moisture transport at all, the surface would be made of sea ice. If we turn on just a bit of $P - E$ (but not so much as to disturb the basic picture), however, then all of the surface would be composed of recycled meteoric ice, which flows toward the equator and is transported back to the poles via the atmosphere.

When $P - E$ becomes strong (**Figure 9**), a sea-ice elevator forms in the tropics; new ice freezes onto the base and is carried upward to the tropical surface, where it sublimates into the atmosphere and eventually falls in the extratropics as snow. This snowfall thickens the extratropical ice in a process compensated partly by basal melting but also by equatorward flow in the ice, which causes the tropical ice again to be thicker than its local equilibrium value (though not so much that basal freezing ceases). Some of the snowfall is eventually transported through the ice to the basal melting region, carrying nutrient-laden surface dust into the ocean.

When the sea glacier does not meet open water in the tropics, it is held back by the backpressure required to meet the boundary condition at both poles, and this limits the flow to a slow creep. The flow rate typically amounts to some tens of meters per year, although the precise value depends strongly on ice temperature through the exponential decrease of ice stiffness with increasing temperature. If we take a typical ice velocity of 20 m year^{-1}, it takes approximately a half million years for ice to make the trip from pole to equator. This gives the order of magnitude of residence time of water in the sea glacier. The time needed for the sea glacier to reach equilibrium starting from thin ice also is on the order of a half million to a million years.

Pollard & Kasting (2005) have studied the thin-ice hypothesis of McKay (2000) within a model incorporating sea-glacier flow and argued that solutions with thin tropical ice could plausibly exist. Warren & Brandt (2006), however, have called into question the assumptions leading to these states. Aside from the questions raised by Warren & Brandt (2006), the low albedo and ease of melting of thin ice would tend to give rise to a narrow hysteresis loop similar to that of the Waterbelt state and might therefore be harder to reconcile with the geological record. This issue has yet to be examined in detail.

The study of sea glaciers is still in its infancy. Among other things, the following extensions have yet to be pursued:

- In current models, the temperature-dependent ice stiffness parameter is allowed to vary with latitude but is approximated as independent of depth. In reality, the cold ice at the surface is stiffer than the warmer ice at the base, leading to differential flow.
- Models so far have been one dimensional (in latitude). There is a need to develop two-dimensional models in latitude and longitude, which could represent the effect of flow around continents and the interaction with land ice sheets. This is a mathematically and physically formidable challenge.

- Basal freezing and melting can reject brine and inject fresh water, respectively, driving an oceanic circulation that redistributes heat, may affect ice thickness, and certainly affects ocean chemistry via the resulting mixing.

Seafloor weathering: formation of carbonate by reaction of silicates in the ocean crust with CO_2-laden seawater

6. SNOWBALL DEGLACIATION

6.1. Limits on CO_2 Accumulation

The most fundamental limit on CO_2 accumulation in the atmosphere is the amount that can be outgassed from Earth's interior over the plausible duration of a Snowball glaciation, less the proportion that is taken up by the ocean. Following Kirschvink, we at first assume that all silicate weathering ceases during a Snowball, so that all outgassed CO_2 accumulates in the atmosphere and ocean. Zhang & Zindler (1993) estimate that the present CO_2 outgassing rate is $2.6 \cdot 10^{12}$ mol year^{-1} and project that it would have been slightly higher (perhaps $3 \cdot 10^{12}$ mol year^{-1}) in the Neoproterozoic. Over 10 million years, the latter figure yields an atmosphere-ocean CO_2 inventory of $3 \cdot 10^{19}$ mol, which would correspond to an atmospheric inventory $p_{I,CO_2} = 253$ mbar, partial pressure $p_{CO_2} = 179$ mbar, or mole fraction 14% if it all stayed in the atmosphere. If the atmosphere and ocean come into equilibrium, however, the fraction that remains in the atmosphere is affected by carbonate/bicarbonate equilibrium in the ocean, which shifts with the CO_2 inventory. At such high values, approximately a third of the CO_2 remains in the atmosphere, as opposed to approximately 3% in modern conditions (Higgins & Schrag 2003). Therefore, a more reasonable estimate of the atmospheric content would be an atmospheric inventory of 10^{19} mol, an atmospheric inventory $p_{I,CO_2} = 85$ mbar, partial pressure $p_{CO_2} = 57$ mbar, or mole fraction 5.3%. All in all, an atmospheric molar concentration of 10%, equivalent to ~100 mbar partial pressure, would be a generous estimate of the amount of CO_2 that could accumulate in the atmosphere during a Snowball episode.

Assuming the atmosphere and ocean to be in equilibrium is reasonable because a substantial fraction of the outgassing is submarine to begin with; moreover, only a small area of open water is required to maintain equilibrium (Le Hir et al. 2008a). As CO_2 builds up, the ocean acidifies, although this is partly buffered by dissolution of seafloor carbonates; the reduction in pH increases the atmospheric fraction. Thus, for a constant outgassing rate during the Snowball, the atmospheric CO_2 rises slowly at first, but the pace accelerates over time. The buffering of the ocean requires an adequate supply of sedimentary carbonate because there is little or no land carbonate weathering during a Snowball. If at some point in the process the sedimentary supply is exhausted, the pH of the ocean goes down more sharply, and the air fraction increases beyond the value given above. This would make deglaciation easier, but it also opens the possibility that once deglaciation starts, the resupply of carbonate ion to the ocean would draw down atmospheric CO_2 and perhaps abort the deglaciation.

Although continental weathering ceases during a Snowball, seafloor weathering continues, and this limits the accumulation of CO_2 (Le Hir et al. 2008a). Assuming an outgassing rate of $7.15 \cdot 10^{12}$ mol year^{-1} (somewhat more than twice the estimate of Zhang & Zindler (1993), Le Hir et al. (2008a) find that p_{CO_2} asymptotes to somewhat less than 300 mbar after 30 million years. This calculation shows that the limits on CO_2 buildup may be stringent, even allowing for a high outgassing rate and a long-duration Snowball. Depending on the behavior of clouds and surface albedo, a p_{CO_2} of 300 mbar may be enough to deglaciate some Neoproterozoic models with CO_2 alone, but for the Makganyene event, when the Sun was much fainter, the limit poses an especially severe problem. The processes governing seafloor weathering are poorly constrained, and the subject requires much further development to see how stringent the upper bound really is. Even

more important, weathering of seafloor basalts provides a supply of carbonate ions that can buffer the ocean pH even after sedimentary carbonates are exhausted. This form of buffering sets in long before CO_2 asymptotes at its equilibrium value.

The analysis of oxygen mass-independent fractionation data by Bao et al. (2009) also puts a cap on the maximum allowable CO_2. The most plausible interpretation of this data implies that the CO_2 levels after the Marinoan glaciation reached no higher than 8% and could have been as low as 1.2%. Many lines of evidence thus point toward the necessity of being able to escape from a Snowball state with atmospheric CO_2 concentrations not exceeding 10%.

CO_2 condensation is another process that could potentially limit the buildup of CO_2 in the atmosphere. On the basis of the Clausius-Clapeyron relation, CO_2 frost forms when p_{CO_2} exceeds 1.8 mbar when the temperature is 140 K, 31 mbar when the temperature is 160 K, and 98 mbar when the temperature is 170 K. The winter polar surface temperatures shown in **Figure 5** fall into this range, so a substantial amount of CO_2 condenses out onto the surface near the winter pole when CO_2 molar concentrations reach ~10%. However, when the pole warms up again in the springtime, the CO_2 frost sublimates back into the atmosphere, leading to a rather Mars-like seasonal cycle of p_{CO_2}. On Mars, polar CO_2 condensation leads to a global seasonal cycle of p_{CO_2} because the atmosphere is practically pure CO_2, so condensation reduces polar surface pressure greatly, creating a pressure gradient large enough to drive a strong convergence of the atmosphere into the polar region. It is not clear that this would happen on a Snowball Earth, where CO_2 would be a relatively minor constituent. On a Snowball Earth, the seasonal cycle of p_{CO_2} might be confined to the polar regions. This is important because a global seasonal cycle of p_{CO_2} would weaken the greenhouse effect at the summer pole and in the tropics, further inhibiting deglaciation. Determination of the global consequences of CO_2 condensation requires simulating CO_2 transport, the effect of latent heat release from the condensation (which limits the maximum condensation rate), and perhaps also the warming effects of CO_2 clouds on the polar night, as has proved important for the early Mars climate (Forget & Pierrehumbert 1997). None of this has been accomplished.

6.2. Deglaciation Criteria

What conditions must be met for a Snowball state to deglaciate? Certainly, a sufficient condition is that the annual mean surface temperature approach the melting point. It is a consequence of Fourier's solution that the seasonal temperature fluctuation dies out within approximately 2 m of the surface (Pierrehumbert 2010, chapter 7); deeper than that, the temperature is the steady diffusive conduction profile corresponding to the annual mean temperature at the surface and to the freezing point of seawater at the base of the ice. When the annual mean surface temperature approaches the freezing point of seawater, the entire ice layer warms up and melts away from below. This is the deglaciation criterion employed in Pierrehumbert (2004, 2005).

Several subtleties, however, could perhaps result in deglaciation even when the annual mean surface temperature is significantly below freezing. One of those processes is the melt-ratchet process, depicted in **Figure 10**, which can operate on either seasonal or diurnal timescales. During the hot part of the season or day, meltwater forms at the surface if the temperature reaches the melting point (in this case, the melting point of the freshwater ice at the surface). Then, if that water is somehow removed—perhaps by drainage through a moulin, as happens when the Greenland ice sheet surface melts, or perhaps through runoff to some distant point, where it collects in a lake—the ice thickness will have been reduced by the amount of the melt. This amount can be considerable, given that relatively little energy is required to melt ice. Then, during the cold part of the day or season, only a small amount of ice can reform if the ice layer is thick because the ice forms at the bottom of the layer, and the rate of formation is limited by the slow diffusion of heat

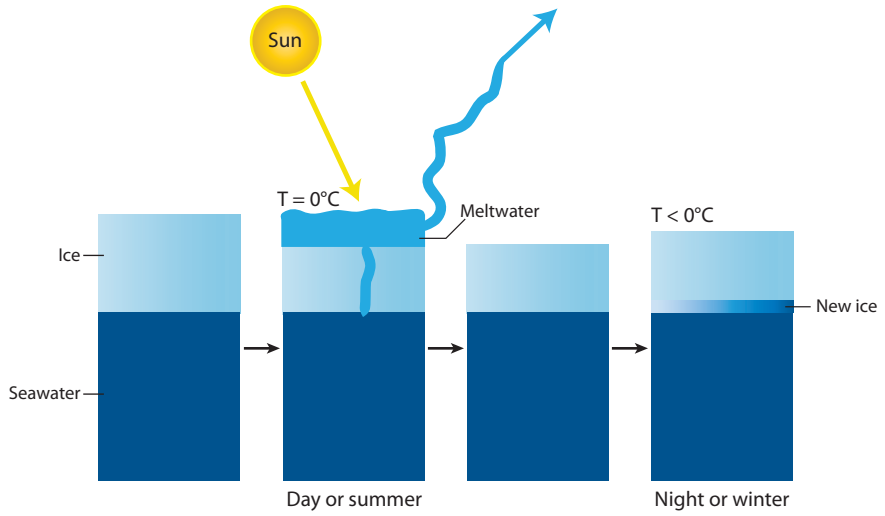

Figure 10

Illustration of the melt-ratchet mechanism for deglaciation with diurnal or annual mean surface temperature below the melting point.

through thick ice. Thus, each cycle leads to some net ablation, which eventually thins the ice to the deglaciation point. The mean temperature over the cycle is well below freezing because the temperature is free to plummet in the night or winter.

Many (perhaps most) GCMs have a spurious melt ratchet, because they teleport away meltwater without regard to whether it can actually leave, where it might go, and what it does when it gets there. Additionally, for the reasons discussed in Section 5, many GCMs exaggerate the diurnal cycle over ice, leading to spurious daytime melting. On the diurnal timescale, it is unlikely that the relatively small amount of meltwater would travel far. In reality, it would most likely remain in the surface or saturate porous snow, and it would prevent nighttime temperatures from falling below freezing until all the surface energy loss was consumed by the latent heat required to refreeze the ice. In this sense, the meltwater would act as a source of additional thermal inertia rather than a form of ablation. A similar process might happen on the seasonal timescale, but in that case, it is more likely that the meltwater would travel a greater distance before meeting its ultimate fate. In any event, to model the ablation properly when the temperature hits the melting point for only a part of the year, one must fully model the meltwater hydrology and account for the energy involved in refreezing the water or for the processes that might allow the water to fracture the ice and drain into the ocean without refreezing. This formidable problem has not been attacked, although the similarities with meltwater hydrology in Greenland (Zwally et al. 2002) should prove helpful. The surface distribution of the meltwater also would have a considerable effect on the albedo of the melting surface, perhaps accelerating the melting significantly. At this point, it is reasonable to conjecture that deglaciation occurs when some portion of the ice surface remains at the melting point for a sufficiently long portion of the year, but the threshold cannot yet be pinned down with any precision.

If solar radiation can deposit its energy a few meters below the ice surface, it, too, can lead to deglaciation, for the same reasons that it can lead to thin ice. Penetration to such depths requires snow-free, clear, bubble-free ice, and even then, proper representation of the process requires fairly high spectral resolution in the computation of radiative transfer in the ice. GCMs that represent

the process at all almost invariably employ crude models with little or no spectral resolution. This can lead to spurious deglaciation.

6.3. Threshold CO_2 for Deglaciation

The first GCM study of Snowball deglaciation revealed that the climate sensitivity is very low in a Snowball state and that even increasing the CO_2 concentration to 10% leaves the planet far short of deglaciation, particularly if the annual mean temperature criterion is employed (Pierrehumbert 2004, 2005). This is well illustrated by the FOAM default-albedo simulations shown in **Figure 11**. The annual mean equatorial surface air temperature increases only from 240 K to 243.6 K as CO_2 concentration is increased from 2,000 ppmv all the way to 10%. The maximum solstice temperatures are only a few degrees higher in this case, so the system is not even close to the point where seasonal melt is generated. These results are somewhat colder than the simulations in Pierrehumbert (2004, 2005) despite the use of a more realistic (and lower) albedo of cold ice in the new simulations because the largely snow-free tropical continent in the earlier simulations warms the tropics.

The main reasons for low climate sensitivity are the weak radiative forcing arising from the weak vertical temperature contrast in the summer hemisphere; the even weaker vertical temperature contrast in the winter hemisphere (which remains cold and bleeds off energy from the summer hemisphere); the absence of water vapor feedbacks in the cold, dry atmosphere; and the weak

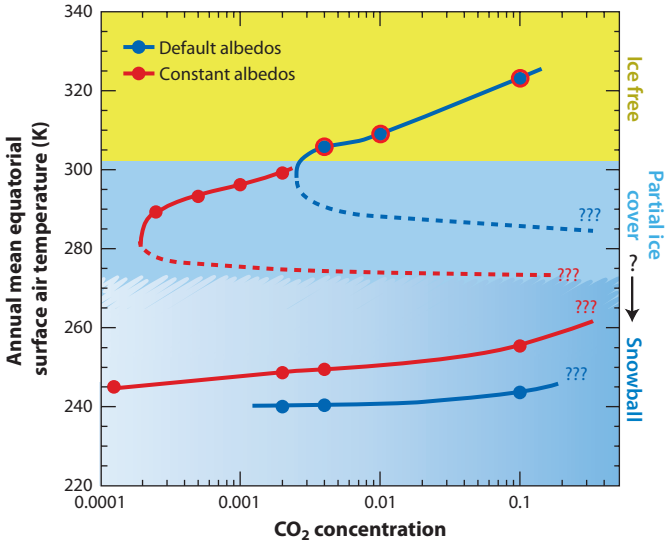

Figure 11

Bifurcation diagram for Fast Ocean Atmosphere Model v1.5 (FOAM) general circulation model simulations with default albedos (*blue dots*) and constant albedos (*red dots*). The two sets of simulations yield identical results when the climate is ice free, so that the red constant-albedo curve continues into the blue default-albedo curve when the climate becomes ice free, as indicated by the red circles surrounding blue dots. Dashed lines represent the position of the unstable branch, which must exist by continuity considerations but was not explicitly computed. The blue shading in the middle of the figure denotes states with partial ice cover, whereas the blue-white band at the bottom denotes Snowball states; the exact position of the boundary between the two regions is uncertain. CO_2 concentrations are given as fractions (e.g., 0.0001 equals 100 ppmv).

cloud feedbacks. The fact that the absorption coefficients of greenhouse gases become weaker at low temperatures also contributes. Many of these factors are tied to the chilling effect of the high-albedo snow cover, which not only cools the climate and means one has farther to go to get to deglaciation, but also reduces the climate sensitivity so that it is harder to get there by increasing CO_2. Many intermodel differences in the deglaciation threshold (e.g., Le Hir et al. 2007) are probably tied to surface-albedo assumptions.

Clouds are another significant unknown affecting deglaciation. As noted in Pierrehumbert (2002), clouds have an unambiguous warming effect on the Snowball climate because the high surface albedo means that the cloud greenhouse effect is not much offset by the cloud albedo effect. Because condensed water is orders of magnitude more effective as an infrared absorber than is water vapor, the cloud greenhouse effect can be important even in very cold situations in which the water vapor greenhouse can be neglected. For example, calculations with the CCM radiation model employed in Section 3 show that introducing tropospheric clouds with ice content that is a mere 1% of the local saturation water vapor content at each altitude reduces the *OLR* by 17 W m^{-2} at a surface temperature of 260 K and 30 W m^{-2} at 270 K. The true cloud cover is modulated by large-scale dynamics (Pierrehumbert 2005), but with regard to parameterizations, the main issues are subgrid-scale fractional cloud cover and the vertical profile of cloud condensed water content; the latter is affected by the vigor of convection and by particle fall speed (controlled largely by size). The FOAM parameterization yields rather weak cloud feedbacks in cold conditions, whereas the LMDz model yields thick tropospheric cirrus clouds, which have a strong warming effect (Le Hir et al. 2007, 2010). There are also indications that CAM has stronger cold cloud feedbacks than FOAM has (see figure 9 of Abbot & Pierrehumbert 2010). The cold convective Snowball ice clouds are driven by moisture advection, condensation settling, and evaporation in a background of essentially dry convective dynamics unaffected by latent heat release. They have no real analog in the modern climate, and standard GCM cloud parameterizations were not designed to deal with them. A proper treatment of such clouds will require much theoretical work, as well as simulations with cloud-resolving models.

6.4. Mudball Earth

It has long been suspected that dust could lower the surface albedo sufficiently to help deglaciate a Snowball state. The problem with dust as a route to deglaciation is that it gets buried quickly by new snow, which limits its impact. However, the peculiar hydrological cycle of the Snowball state, with its net ablation zone in the tropics and global sea-glacier flow converging ice into that region, provides a way around this dilemma. The flow and ablation results in nearly all the dust that falls globally in the course of a Snowball accumulating in a dust moraine in the tropics. Modeling has confirmed that this process easily can trigger deglaciation at CO_2 concentrations below 10% (Abbot & Pierrehumbert 2010). We think that the Mudball, perhaps abetted by somewhat stronger cloud feedbacks than FOAM produces and by the warming effect of dust aerosols (Abbot & Halevy 2010), provides the most viable route to deglaciating a Snowball. The Mudball hypothesis does not obviate the role of CO_2 accumulation; the warming from CO_2 is still one of the pacemakers that primes the planet for deglaciation, although the timescale for accumulation of the dust moraine does not differ greatly from the timescale for CO_2 accumulation.

7. THE SNOWBALL AFTERMATH

A fully consistent calculation of deglaciation incorporating realistic ice thickness, realistic atmospheric transports, and sea-glacier flow has not been carried out, but simple energy budget

considerations indicate that once deglaciation of a Snowball begins, it proceeds rapidly to a globally ice-free state. High CO_2 in conjunction with the low albedo of open water bathes the ice in hot air and laps it with warm water, which easily drives a substantial energy flux into the ice. A mere 10 W m^{-2} would melt through a 700-m ice layer in 740 years, so that even if the flux were applied only within 1,000 km of the ice margin, the globe would deglaciate in 7,400 years. In reality, once substantial surface meltwater ponds form, fracturing and even more rapid disintegration of the ice cover likely ensue, as happened for the Larsen B Ice Shelf (Scambos et al. 2000). This leaves Earth with high CO_2 and a low-albedo surface, leading to the postglacial hothouse. Space permits only a brief discussion of the postglacial hothouse, which has, in any event, not been studied extensively.

The rapid melt leaves behind a hot freshwater cap several hundred meters thick above a briny ocean. The rate at which this layer mixes away and the way in which it affects the postglacial depositional environment for cap carbonate sequences represent major unsolved problems of Neoproterozoic oceanography.

Allen & Hoffman (2005) argue that formation of giant wave ripples requires prevailing surface winds in excess of 20 m s^{-1} and propose that this is a signature of the large temperature gradient between the ice edge and the hot ocean during the deglaciation stage. However, the thermal wind relation links surface temperature gradients to large winds aloft—not at the surface. Strong prevailing surface winds involve more complex fluid dynamical processes. In the tropics, they would arise from a greatly enhanced Hadley circulation; in the midlatitudes, from greatly enhanced synoptic eddy momentum convergence. Whether either of these mechanisms can produce surface winds of the required strength is not clear, but the matter requires further study. If giant wave ripples can be produced by individual storms rather than by steady prevailing winds, the extreme amplification of hurricane intensity arising from the hot ocean provides an easy way to produce the required winds. One would expect the giant wave ripples, then, to persist throughout the postglacial hothouse because hurricanes do not draw their energy from horizontal temperature contrasts.

The equatorial temperature of the postglacial hothouse can be read off the upper branch of **Figure 11**. These states have a fairly weak meridional temperature gradient, with polar temperatures only ~20 K lower than those in the tropics. If the CO_2 reaches 10% upon deglaciation, the postglacial tropical oceans reach 323 K in the FOAM simulations. This is not nearly sufficient to sterilize the tropical ocean, and, in any event, the polar ocean temperature is hardly greater than the modern tropics. The postglacial hothouse presents a not terribly narrow biological bottleneck, preventing the survival of marine taxa that require temperatures significantly lower than those found in the modern tropics. Simulations with tropical continents (not shown) produce much more threatening temperatures over land, but given that there was no complex land life in the Neoproterozoic, the high land temperature is of uncertain importance.

The time required for the postglacial hothouse to recover to more normal temperatures was studied by Le Hir et al. (2008b), who used a coupled GCM/geochemical model. The rainfall rate over land is one of the key factors controlling silicate weathering rates, and as predicted theoretically in Pierrehumbert (2002), the rainfall rate in the hothouse is not nearly as high as one would expect from the Clausius-Clapeyron exponential scaling with temperature. The limitation occurs because it is difficult to increase rainfall beyond the point where nearly all the available solar radiation reaching the surface is used to evaporate water. The limited precipitation results in a much longer duration of the postglacial hothouse than was previously estimated. The recovery time also was found to be highly sensitive to assumptions about effective weatherable area, which, in turn, is tied to the depth of the moistened soil layer and typical silicate grain size. Over a plausible range of these parameters, the CO_2 concentration drops from an initial value of 12% to between 0.6% (6,000 ppmv) and 3% after 1 million years. In the highest surface area case, the

concentration has fallen to 1,500 ppmv after 3 million years and is near equilibrium, but in the lowest surface area case, the concentration is still above 1% after 10 million years and has not yet equilibrated. Note that the time over which cap dolostones are laid down is expected to be much shorter than the duration of the postglacial hothouse because cap dolostones are limited by the supply of easily weatherable land carbonates. In contrast, silicate weathering of the isotopically light excess carbon in the atmosphere-ocean system produces a slower deposition that persists throughout the postglacial hothouse.

8. CONCLUSIONS AND PROSPECTS

From the standpoint of basic climate dynamics, GCM experiments show that there is no particular barrier to initiation of a Snowball state at plausible CO_2 concentrations under Neoproterozoic conditions. Entry in a plausible CO_2 range does, however, depend crucially on the increase of albedo due to snow cover. Moreover, recent simulations confirm earlier indications that dynamical ocean heat transport inhibits Snowball glaciation and drives the CO_2 threshold for initiation to lower values; this subject has still not been extensively explored, and it is well within the bounds of possibility that ocean dynamic effects could drive the threshold to values that are geochemically difficult to attain. Finding a plausible way to get out of a Snowball is more difficult. Surface albedo is a critical factor here, too, but beyond that, it looks as though deglaciating a Neoproterozoic Snowball through CO_2 accumulation alone would be difficult to accomplish. This is certainly true if the cloud greenhouse effect is weak, but one cannot rule out a stronger cloud feedback on thermodynamic grounds alone, and that means it is important to come to some understanding of the nature of clouds in the cold, convective Snowball regime. With only modest help from clouds, though, the Mudball mechanism provides a viable exit strategy, although the hypothesis requires much further study.

Both the initiation and the deglaciation problems require a better understanding of the nature of the ice and snow surface—regarding its albedo and the hydrology of surface meltwater.

There seems to be a prevailing notion that Waterbelt states are the default hypothesis for Neoproterozoic glaciation and that more extraordinary evidence should be required in support of a Snowball than in support of a Waterbelt. As a result, little effort has been expended on quantifying the biogeochemical consequences of a Waterbelt. To us, the Waterbelt seems, if anything, more implausible than a Snowball because the idea that Earth would sit on the precipice of global glaciation for millions of years without falling off defies credibility. Waterbelt states can certainly exist, from the standpoint of basic climate dynamics, but the question is whether they can be made compatible with the geological record. In particular, credible, quantitative modeling is needed to resolve the following issues:

- Are active tropical land ice sheets compatible with a Waterbelt state? So far, this issue has been examined only within EBMs that offer almost infinite scope for ad hoc adjustments to precipitation.
- Can banded iron formations be deposited during a Waterbelt state?
- Can Waterbelt states be reconciled with cap carbonates, extreme CO_2 accumulation, and other indicators of a wide hysteresis loop?

Explaining the geochemical picture of the Neoproterozoic, and how it relates to the initiation of glaciations, presents a continuing and largely unmet challenge. Snowball glaciations, and low-latitude glaciations in general, represent a breakdown of the silicate weathering thermostat. This breakdown probably involves both the organic and inorganic parts of the carbon cycle, and likely methanogenesis, methanotrophy, and sulfate reduction as well. The keystone of the problem is

explaining the *preglacial* negative ^{13}C excursions, and how the nonglacial Shuram excursion relates to the preglacial Marinoan and Sturtian excursions. It is crucial to settle the existence of a highly available organic carbon pool, such as that proposed by Rothman et al. (2003), and to resolve the compatibility of such a pool with sulfate reduction and the redox budget of Earth. Insofar as methanogenesis is central to the anaerobic decomposition of small organic molecules, fluctuations in methanogenesis may play a role in the stocking and destocking of organic carbon, in addition to affecting the atmosphere's methane concentration. If preglacial negative excursions result from conventional reductions in the organic carbon burial proportion, without involving destocking of an organic carbon pool, there is still the need to explain why the fluctuations occur, the magnitude of associated CO_2 accumulation and warming, and whether subsequent glaciations are in some way a consequence of the warm phase. There is also a critical need for interglacial Neoproterozoic temperature proxies, if there is to be any hope for testing hypotheses about the connection between the carbon cycle and atmospheric greenhouse gas concentration.

The essential puzzle of the Neoproterozoic can be summed up in three questions: What happened during the Neoproterozoic to terminate the Boring Billion? How inevitable was it that this should have occurred? Could the Boring Billion have become the Boring Four Billion, depriving curious metazoans of the enjoyment of pondering such questions?

DISCLOSURE STATEMENT

The authors are not aware of any affiliations, memberships, funding, or financial holdings that might be perceived as affecting the objectivity of this review.

ACKNOWLEDGMENTS

The authors are indebted to Francis MacDonald, David Fike, Adam Maloof, Paul Hoffman, and Lou Derry for many illuminating communications regarding the geological record of the Neoproterozoic and its interpretation. R.T.P. is particularly grateful to Paul Hoffman and Dan Schrag for introducing him to Snowball Earth. Jonathan Mitchell and Xavier Levine carried out the radiative-convective seasonal cycle simulations discussed in Section 5 and kindly provided access to their as-yet unpublished results. Jochem Marotzke provided much valuable guidance regarding simulations carried out with the ECHAM and MPI models. Chris Walker provided technical assistance for the CAM simulations. R.T.P. and D.S.A. are grateful for the support of the Canadian Institute for Advanced Research. D.S.A. was also supported the T.C. Chamberlin Fellowship of the University of Chicago, and D.K. was supported by the Harvard College Research Program and by the U.S. National Science Foundation (NSF) P2C2 program (ATM-0902844). The work of A.V. was supported by the Max Planck Society and the International Max Planck Research School on Earth System Modeling. The ECHAM5 simulations were performed at the German Climate Computing Center (DKRZ) in Hamburg, Germany. The Neoproterozoic Climate group at the University of Chicago is funded in part by the NSF under award AGS0933936.

LITERATURE CITED

Abbot DS, Eisenman I, Pierrehumbert RT. 2010. The importance of ice vertical resolution for Snowball climate and deglaciation. *J. Clim.* 23:6100–9

Abbot DS, Halevy I. 2010. Dust aerosol important for Snowball Earth deglaciation. *J. Climate* 23:4121–32

Abbot DS, Pierrehumbert RT. 2010. Mudball: surface dust and Snowball Earth deglaciation. *J. Geophys. Res.* 115:D03104

Allen PA, Hoffman PF. 2005. Extreme winds and waves in the aftermath of a Neoproterozoic glaciation. *Nature* 433:123–27
Bao H, Fairchild IJ, Wynn PM, Spotl C. 2009. Stretching the envelope of past surface environments: Neoproterozoic glacial lakes from Svalbard. *Science* 5910:119–22
Berner RA. 2004. *The Phanerozoic Carbon Cycle: CO_2 and O_2*. New York: Oxford Univ. Press
Bodiselitsch B, Koeberl C, Master S, Reimold WU. 2005. Estimating duration and intensity of Neoproterozoic Snowball glaciations from Ir anomalies. *Science* 308:239–42
Brady PV, Caroll SA. 1994. Direct effects of CO_2 and temperature on silicate weathering: possible implications for climate control. *Geochim. Cosmochim. Acta* 58:1843–56
Bristow TF, Kennedy MJ. 2008. Carbon isotope excursions and the oxidant budget of the Ediacaran atmosphere and ocean. *Geology* 36:863–66
Budyko MI. 1969. The effect of solar radiation variations on the climate of the Earth. *Tellus* 21:611–19
Caballero R, Mitchell J, Pierrehumbert RT. 2008. Axisymmetric, nearly inviscid circulations in noncondensing radiative-convective atmospheres. *Q. J. R. Meteorol. Soc.* 134:1269–85
Caldeira K, Kasting JF. 1992. Susceptibility of the early Earth to irreversible glaciation caused by carbon dioxide clouds. *Nature* 359:226–28
Canfield DE. 2005. The early history of atmospheric oxygen: homage to Robert M. Garrels. *Annu. Rev. Earth Planet. Sci.* 33:1–36
Collins WD, Rasch PJ, Boville BA, Hack JJ, McCaa JR, et al. 2004. Description of the NCAR Community Atmosphere Model (CAM 3.0). *NCAR Tech. Note*, Natl. Cent. Atmos. Res., Boulder, Colo.
Crowley TJ, Baum SK. 1993. Effect of decreased solar luminosity on Late Precambrian ice extent. *J. Geophys. Res.* 98:16723–32
Crowley TJ, Hyde WT, Peltier WR. 2001. CO_2 levels required for deglaciation of a "near-snowball" Earth. *Geophys. Res. Lett.* 28:283–86
Derry LA. 2010. A burial diagenesis origin for the Ediacaran Shuram-Wonoka carbon isotope anomaly. *Earth Planet. Sci. Lett.* 294:152–62
Donnadieu Y, Fluteau F, Ramstein G, Ritz C, Besse J. 2003. Is there a conflict between the Neoproterozoic glacial deposits and the snowball Earth interpretation: an improved understanding with numerical modeling. *Earth Planet. Sci. Lett.* 208:101–12
Donnadieu Y, Godderis Y, Pierrehumbert RT, Dromart G, Fluteau F, Jacob R. 2006. A GEOCLIM simulation of climatic and biogeochemical consequences of Pangea breakup. *Geochem. Geophys. Geosyst.* 7:Q11019
Donnadieu Y, Ramstein G, Fluteau F, Roche D, Ganopolski A. 2004. The impact of atmospheric and oceanic heat transports on the sea-ice-albedo instability during the Neoproterozoic. *Clim. Dyn.* 22:293–306
Fairchild IJ, Kennedy MJ. 2007. Neoproterozoic glaciation in the Earth System. *J. Geol. Soc.* 164:895–921
Fike DA, Grotzinger JP, Pratt LM, Summons RE. 2006. Oxidation of the Ediacaran ocean. *Nature* 444:744–47
Forget F, Pierrehumbert RT. 1997. Warming early Mars with carbon dioxide clouds that scatter infrared radiation. *Science* 278:1273–76
Godderis Y, Donnadieu Y, Nédélec A, Dupré B, Dessert C, et al. 2003. The Sturtian 'snowball' glaciation: fire and ice. *Earth Planet. Sci. Lett.* 211:1–12
Goodman GC. 2006. Through thick and thin: marine and meteoric ice in a "Snowball Earth" climate. *Geophys. Res. Lett.* 33:L16701
Goodman JC, Pierrehumbert RT. 2003. Glacial flow of floating marine ice in "Snowball Earth." *J. Geophys. Res.* 108(C10):3308
Gough DO. 1981. Solar interior structure and luminosity variations. *Sol. Phys.* 74:21–34
Haqq-Misra JD, Domagal-Goldman SD, Kasting PJ, Kasting JF. 2008. A revised, hazy methane greenhouse for the Archean Earth. *Astrobiology* 8:1127–37
Hayes JM, Waldbauer JR. 2006. The carbon cycle and associated redox processes through time. *Philos. Trans. R. Soc. B* 361:931–50
Higgins JA, Schrag DP. 2003. Aftermath of a snowball Earth. *Geochem. Geophys. Geosyst.* 4:1028
Hoffman PF, Halverson GP, Domack EW, Husson JM, Higgins JA, Schrag DP. 2007. Are basal Ediacaran (635 Ma) post-glacial "cap dolostones" diachronous? *Earth Planet. Sci. Lett.* 258:114–31
Hoffman PF, Kaufman AJ, Halverson GP, Schrag DP. 1998. A Neoproterozoic snowball Earth. *Science* 281:1342–46

Hoffman PF, Li Z-X. 2009. A palaeogeographic context for Neoproterozoic glaciation. *Palaeogeogr. Palaeoclimatol. Palaeoecol.* 277:158–172

Hoffman PF, Schrag DP. 2002. The snowball Earth hypothesis: testing the limits of global change. *Terra Nova* 14:129–55

Hyde WT, Crowley TJ, Baum SK, Peltier WR. 2000. Neoproterozoic 'snowball Earth' simulations with a coupled climate/ice-sheet model. *Nature* 405(6785):425–29

Jacob R. 1997. *Low frequency variability in a simulated atmosphere-ocean system*. PhD thesis. Univ. Wis. Madison. 170 pp.

Jiang G, Kennedy MJ, Christie-Blick N. 2003. Stable isotopic evidence for methane seeps in Neoproterozoic postglacial cap carbonates. *Nature* 426:822–26

Kappler A, Pasquero C, Konhauser KO, Newman DK. 2005. Deposition of banded iron formations by anoxygenic phototrophic Fe(II)-oxidizing bacteria. *Geology* 33:865–68

Kennedy M, Mrofka D, von der Borch C. 2008. Snowball Earth termination by destabilization of equatorial permafrost methane clathrate. *Nature* 453:642–45

Kiehl JT, Briegleb B. 1992. Comparison of the observed and calculated clear sky greenhouse-effect: implications for climate studies. *J. Geophys. Res.* 97(D9):10037–49

Kiehl JT, Hack JJ, Bonan GB, Boville BA, Williamson DL, Rasch PJ. 1998. The National Center for Atmospheric Research Community Climate Model: CCM3. *J. Clim.* 11:1131–49

Kirschvink JL. 1992. Late Proterozoic low-latitude global glaciation: the snowball Earth. In *The Proterozoic Biosphere: A Multidisciplinary Study*, ed. JW Schoff, C Klein, pp. 51–52. New York: Cambridge Univ. Press

Laskar J. 1996. Large scale chaos and marginal stability in the solar system. *Celest. Mech. Dyn. Astron.* 64:115–62

Le Hir G, Ramstein G, Donnadieu Y, Pierrehumbert RT. 2007. Investigating plausible mechanisms to trigger a deglaciation from a hard snowball Earth. *C. R. Geosci.* 339(3–4):274–87

Le Hir G, Ramstein G, Donnadieu Y, Godderis Y. 2008a. Scenario for the evolution of atmospheric pCO_2 during a snowball Earth. *Geology* 36:47–50

Le Hir G, Donnadieu Y, Godderis Y, Pierrehumbert RT, Halverson GP, et al. 2008b. The snowball Earth aftermath: exploring the limits of continental weathering processes. *Earth Planet. Sci. Lett.* 277:453–63

Le Hir G, Donnadieu Y, Krinner G, Ramstein G. 2010. Toward the snowball earth deglaciation. *Clim. Dyn.* 35:285–97

Levrard B, Laskar J. 2003. Climate friction and the Earth's obliquity. *Geophys. J. Int.* 154:970–90

Lewis JP, Weaver AJ, Johnston ST, Eby M. 2003. Neoproterozoic "snowball Earth": dynamic sea ice over a quiescent ocean. *Paleoceanography* 18(4):1092

Li ZX, Bogdanova SV, Collins AS, Davidson A, De Waele B, et al. 2008. Assembly, configuration, and break-up history of Rodinia: a synthesis. *Precambrian Res.* 160:179–210

Love G, Grosjean E, Stalvies C, Fike DA, Grotzinger JP, et al. 2009. Fossil steroids record the appearance of Demospongiae during the Cryogenian period. *Nature* 457:718–21

Macdonald FA, Schmitz MD, Crowley JL, Roots CF, Jones DS, et al. 2009. Calibrating the Cryogenian. *Science* 327:1241–43

Marotzke J, Botzet M. 2007. Present-day and ice-covered equilibrium states in a comprehensive climate model. *Geophys. Res. Lett.* 34:L16704

Marsland SJ, Haak H, Jungclaus JH, Latif M, Roske F. 2003. The Max-Planck-Institute global ocean/sea ice model with orthogonal curvilinear coordinates. *Ocean Model.* 5(2):91–127

McCaa J, Rothstein M, Eaton B, Rosinski J, Kluzek E, Vertenstein M. 2004. *User's guide to the NCAR Community Atmosphere Model (CAM 3.0)*. **http://www.cesm.ucar.edu/models/atm-cam/docs/usersguide/**

McKay CP. 2000. Thickness of tropical ice and photosynthesis on a snowball Earth. *Geophys. Res. Lett.* 27:2153–56

McKay CP, Lorenz RD, Lunine JI. 1999. Analytic solutions for the antigreenhouse effect: Titan and the early Earth. *Icarus* 137:56–61

Micheels A, Montenari M. 2008. A snowball Earth versus a slushball Earth: results from Neoproterozoic climate modeling sensitivity experiments. *Geosphere* 4(2):401–10

Mitchell J. 2008. The drying of Titan's dunes: Titan's methane hydrology and its impact on atmospheric circulation. *J. Geophys. Res.* 113:E08015

Pavlov AA, Hurtgen MT, Kasting JF, Arthur MA. 2003. Methane-rich Proterozoic atmosphere? *Geology* 31:87–90

Pavlov AA, Kasting JF, Brown LL, Rages KA, Freedman R. 2000. Greenhouse warming by CH_4 in the atmosphere of early Earth. *J. Geophys. Res.* 105(E5):11981–90

Pierrehumbert RT. 2002. The hydrologic cycle in deep-time climate problems. *Nature* 419:191–98

Pierrehumbert RT. 2004. High levels of atmospheric carbon dioxide necessary for the termination of global glaciation. *Nature* 429:646–49

Pierrehumbert RT. 2005. Climate dynamics of a hard snowball Earth. *J. Geophys. Res.* 110:D01111

Pierrehumbert RT. 2010. *Principles of Planetary Climate*. New York: Cambridge Univ. Press

Pollard D, Kasting JF. 2005. Snowball Earth: a thin-ice solution with flowing sea glaciers. *J. Geophys. Res.* 110:C07010

Poulsen CJ, Jacob RL. 2004. Factors that inhibit snowball Earth simulation. *Paleoceanography* 19:PA4021

Poulsen CJ, Pierrehumbert RT, Jacob RL. 2001. Impact of ocean dynamics on the simulation of the Neoproterozoic "snowball Earth." *Geophys. Res. Lett.* 28:1575–78

Pruss SB, Bosak T, Macdonald FA, McLane M, Hoffman PF. 2010. Microbial facies in a Sturtian cap carbonate, the Rasthof Formation, Otavi Group, northern Namibia. *Precambrian Res.* 181:187–98

Ridgwell AJ, Kennedy MJ, Caldeira K. 2003. Carbonate deposition, climate stability, and Neoproterozoic ice ages. *Science* 302:859–62

Roe GH, Baker MB. 2010. Notes on a catastrophe: a feedback analysis of snowball earth. *J. Clim.* 23:4694–703

Roeckner E, Bäuml G, Bonaventura L, Brokopf R, Esch M, et al. 2003. The atmospheric general circulation model ECHAM5, part I: model description. *Tech. Rep. 349*, Max-Planck-Inst. Meteorol., Hambg., Ger.

Rose BEJ, Marshall J. 2009. Ocean heat transport, sea ice, and multiple climate states: insights from energy balance models. *J. Atmos. Sci.* 66:2828–43

Rothman DH, Hayes JM, Summons RE. 2003. Dynamics of the Neoproterozoic carbon cycle. *Proc. Natl. Acad. Sci. USA* 100:8124–29

Scambos TA, Hulbe C, Fahnestock M, Bohlander J. 2000. The link between climate warming and break-up of ice shelves in the Antarctic Peninsula. *J. Glaciol.* 46(154):516–30

Schmidt PW, Williams GE. 1995. The Neoproterozoic climatic paradox: equatorial palaeolatitude for Marinoan glaciation near sea level in South Australia. *Earth Planet. Sci. Lett.* 134:107–24

Schrag DP, Berner RA, Hoffman PF, Halverson GP. 2002. On the initiation of a snowball Earth. *Geochem. Geophys. Geosyst.* 3:1036

Sellers WD. 1969. A global climatic model based on the energy balance of the Earth-atmosphere system. *J. Appl. Meteorol.* 8:392–400

Shields GA. 2005. Neoproterozoic cap carbonates: a critical appraisal of existing models and the *plumeworld* hypothesis. *Terra Nova* 17:299–310

Solomon S, ed. 2007. *Climate Change 2007, the Physical Science Basis: Working Group I Contribution to the Fourth Assessment Report of the Intergovernmental Panel on Climate Change*. Cambridge: Cambridge Univ. Press

Swanson-Hysell NL, Rose CV, Calmet CC, Halverson GP, Hurtgen MT, Maloof AC. 2010. Cryogenian glaciation and the onset of carbon-isotope decoupling. *Science* 328:608–11

Trainer MG, Pavlov AA, DeWitt HL, Jimenez JL, McKay CP, et al. 2006. Organic haze on Titan and the early Earth. *Proc. Natl. Acad. Sci. USA* 103:18035–42

Trindade RIF, Font E, D'Agrella-Filho MS, Nogueira ACR, Riccomini C. 2003. Low-latitude and multiple geomagnetic reversals in the Neoproterozoic Puga cap carbonate, Amazon craton. *Terra Nova* 15:441–46

Trindade RIF, Macouin M. 2007. Palaeolatitude of glacial deposits and palaeogeography of Neoproterozoic ice ages. *C. R. Geosci.* 339:200–11

Voigt A, Abbot DS, Pierrehumbert RT, Marotzke J. 2010. Initiation of a Marinoan Snowball Earth in a state-of-the-art atmosphere-ocean general circulation model. *Clim. Past Discuss.* 6:1853–94

Voigt A, Marotzke J. 2010. The transition from the present-day climate to a modern Snowball Earth. *Clim. Dyn.* 35:887–905

Waldbauer JR, Sherman LS, Sumner DY, Summons RE. 2009. Late Archean molecular fossils from the Transvaal Supergroup record the antiquity of microbial diversity and aerobiosis. *Precambrian Res.* 169:28–47

Walker JCG. 2001. Strange weather on snowball Earth. Presented at Earth Syst. Process. Glob. Meet., June 24–28, Edinb.

Warren SG, Brandt RE. 2006. Comment on "Snowball Earth: a thin-ice solution with flowing sea glaciers" by David Pollard and James F. Kasting. *J. Geophys. Res.* 111:C09016

Warren SG, Brandt RE, Grenfell TC, McKay CP. 2002. Snowball Earth: ice thickness on the tropical ocean. *J. Geophys. Res.* 107(C10):3167

Xiao SH, Knoll AH. 2000. Phosphatized animal embryos from the Neoproterozoic Doushantuo Formation at Weng'An, Guizhou, South China. *J. Paleontol.* 74:767–88

Yung YL, DeMore WB. 1999. *Photochemistry of Planetary Atmospheres*. Oxford: Oxford Univ. Press

Zhang YX, Zindler A. 1993. Distribution and evolution of carbon and nitrogen in Earth. *Earth Planet. Sci. Lett.* 117:331–45

Zwally HJ, Abdalati W, Herring T, Larson K, Saba J, Steffen K. 2002. Surface melt–induced acceleration of Greenland ice-sheet flow. *Science* 297:218–22

Annual Review
of Earth and
Planetary Sciences
Volume 39, 2011

Contents

Indexes

Errata

An online log of corrections to *Annual Review of Earth and Planetary Sciences* articles may be found at http://earth.annualreviews.org